Synthesis and Characterization of Bismuth Sodium Titanate-Barium Titanate Ceramics

A thesis submitted in partial fulfilment of the requirements for the award of

Degree of

Master of Science

In

Physics

Submitted by

Anjali Mehta

Reg. No. 301704036

Under the guidance of

Dr. Poonam Uniyal
Associate Professor

School of Physics and Materials Science
Thapar Institute of Engineering and Technology,
Patiala-147001, Punjab
July, 2019

CERTIFICATE

I, hereby declare that the work which has been presented in this dissertation entitled **"Synthesis and Characterization of Bismuth Sodium Titanate-Barium Titanate Ceramics"** is an authentic record of my own work carried out for the partial fulfilment of the requirement for the award of the degree of Masters of Science in Physics at Thapar Institute Of Engineering And Technology, Patiala (Punjab), under the guidance of **Dr. Poonam Uniyal,** Associate Professor, School of Physics and Materials Science. The intellectual content of this dissertation is the product of my own work and contains no material which to a substantial extent has been accepted for the award of any other degree at this or any other educational institution, except where due acknowledgment is made in the dissertation.

Anjali Mehta

(Anjali Mehta)

Date: 15/07/2019

Roll no. 301704036

Place:

It is to certify that the above statement made by the candidate is correct and true to the best of my knowledge and belief.

Dr. Poonam Uniyal
Associate Professor
SPMS,
Thapar Institute of Engineering and Technology, Patiala

ACKNOWLEDGEMENT

Work on this dissertation would not have been possible without the encouragement and the support of many people. I would like to express my sincere gratitude especially to the following:

The first and greatest thank to my supervisor Dr. Poonam Uniyal for his continuous support and supervision, for his excellent guidance, patience, motivation and enthusiasm.

I would like to thank Dr. O.P Pandey, Professor and Head, SPMS for providing me with an excellent atmosphere and all the necessary facilities for my research. Besides, my supervisor, I would like to thank from the bottom of my heart, Mrs. Kamaldeep Kaur for sharing their valuable experiences. I would not have been able to complete my dissertation without their cooperation.

I would like to acknowledge my lab mate Prinka rani who supported me at each step.

I would like to thank my friends Anushka, Nehal, Harmeet, Anjali, Komal, Rajni, and Navneet being their always with me.

Last but not the least; I would like to thank my father, Mr. Raj Kumar; my mother, Mrs. Anju; and my younger brother Rajat Mehta for their unconditional support, both financially and emotionally throughout my degree.

Above all I render my gratitude to the almighty who bestowed upon me the strength and vision to walk on the path of truth.

Dedicated to my beloved Parents and Grandparents

TABLE OF CONTENTS

LIST OF FIGURES

LIST OF TABLES

LIST OF SYMBOLS AND ABBREVIATIONS

ABBREVIATIONS	FULL FORMS
BT	Barium Titanate, $BaTiO_3$
PZT	Lead Zirconate Titanate
NBT	Sodium Bismuth Titanate, $Bi_{0.5}Na_{0.5}TiO_3$
T_c	Curie temperature
P_r	Remanent polarization
E_c	Coercive field
MPB	Morphotropic Phase Boundary
d_{33}	Piezoelectric coefficient
XRD	X-ray Diffraction
SEM	Scanning Electron Microscopy
θ	Diffraction angle
DX	Energy dispersive X-ray spectroscopy
$\tan\delta$	Dielectric loss
a	Lattice parameter
λ	Wavelength
ε_r	Dielectric constant
Z'	real part of impedance
Z"	imaginary part of impedance
(P_s)	Spontaneous polarization
$\mathcal{E}_o$	Permittivity of free space (8.85×10^{-12} F/m)

Abstract

Ferroelectric ceramics have always been a area of huge attention, in the era of science.These ceramics have pyroelectric, piezoelectric, dielectric and ferroelectric properties which make them suitable for multifunctional device applications. Among the lead-free ferroelectric ceramics, $(Na_{0.5}Bi_{0.5})TiO_3$(NBT) has extremely good properties with a relatively large P_r (~ 38μC/cm^2) and a high E_c (~ 73 kV/cm), high Curie temperature T_c ~320 °C with diffuse phase transition and a moderate piezoelectric coefficient (d_{33}) ~73pC/N.

In the present work, (1-x) $(Bi_{0.5}Na_{0.5})TiO_3$ (BNT) - x $BaTiO_3$ (BT) where (x= 0, 0.1, 0.2, 0.3) ceramics were prepared via solid-state reaction method. X-ray diffraction pattern revealed the perovskite phase with small amount of secondary phase $Na_{0.5}Bi_{4.5}Ti_4O_{15}$.The SEM micrograph show ed dense microstructure and non-uniform grain size. Dielectric and impedance properties of the samples were measured at temperatures ranging from (50 ℃ to 500 ℃) at various applied frequency ranging from 100Hz to 1MHz.

CHAPTER 1
INTRODUCTION

In today's era of device miniaturization, novel ceramic materials are gaining attention and are widely utilized in sensors, memory,resonators, transducer, and capacitor devices. These ceramic materials alter their physicochemical features under the impact of outside stimuli. Because of their unique properties, these materials are also known as electroceramics. A simultaneous development in electroceramics with interesting ferroelectric properties paves a new pathway along with the progress of new technologies. In the electronics industry and other related sectors, these ceramic compounds are widely used because they have high dielectric constant. Moreover, most of the materials with high dielectric constant contains lead in a major proportion which negatively impacts human health and environment due to high toxicity levels of a lead oxide such as lead-zirconium titanate ceramic, PZT **[**1**].** In addition to this, the handling of lead during the manufacturing process is a tedious task as it requires high vapour pressure**.**The direct consumption of lead by human bodies results in severe diseases like blood clotting, neurological disorders and heart-related issues **[**2**].** Addressing the aforementioned issues, some countries have even banned the utilization of lead-based devices. To overcome problems related to lead-based materials, more eco-friendly materials are gaining attraction. So,there is a need to build up lead-free ferroelectric ceramics with tremendous ferroelectric and piezoelectric performance to overcome the issue of environmental degradation and the health of human beings **[**3**].** Perovskite, a lead free ferroelectric material has wide applications in electronic industry such as capacitors and high energy storage devices. The ferroelectric properties of Non-perovskite Bismuth layered structure ferroelectrics (BLSFs) are weak as compared to their perovskite counterparts, yet they possess the superior polarization fatigue endurance property.

1.1 Dielectrics

Dielectrics are the insulating materials, which have no free charge carriers. But the special characteristic of dielectrics is the induction of polarization in the dielectric material under an applied external electric field. As electric field is applied to these materials, the negative charges get displaced reverse to the applied field direction and positive charges are displaced along the field direction. Therefore the creation of the electric dipoles in the field direction is known as

dielectric polarization. This polarization in a dielectric material can occur by several phenomena [4].

Ionic polarization: When the displacement of charged ion occurs comparative to rest ions under influence of the applied electric field. This is known as ionic polarization.

Electronic polarization: Electronic polarization occurs due to a dislocation of the electron cloud of an atom from its a nucleus under an external electric field.

Dipolar or Orientation polarization: Dipolar polarization arises when the permanent dipolesget alignedin presence of an applied field.

Space charge polarization: When the charges get accumulated at the surface of the material, space charge polarization is induced, and diffusion of ions along the electric field gives the redistribution of charges in the dielectric medium.

1.1.1 Frequency dependence of dielectric constant

Owing to irregular distribution, the dielectric material shows decrease in the permittivity (ε) when applied field frequency is increased as shown in Figure 1.1.With the appliance of an electric field (frequency $\leq 10^6$ Hz), electric dipoles of the dielectric material gets oriented. As applied electric field frequency is increased from 10^6 to 10^{11} Hz, polarization drops back with field also the orientational polarization halts.Therefore permittivity changes, while ionic and electronic polarization present.

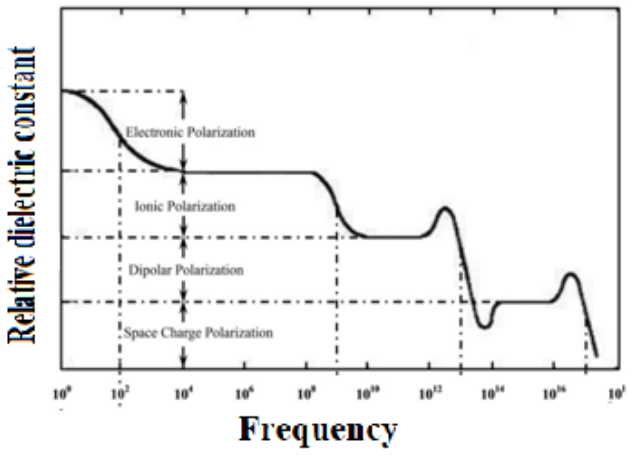

Figure 1.1: Frequency dependence of different polarizations [5]

The +ve as well as the –ve ions of the material doesn't go well with the variations of the field,when there is increase in the frequency from 10^{11} Hz to 10^{14} Hz. This results in halt of ionic

polarization and there is change in the value of dielectric constant as well. The existence of electronic polarization is up to 10^{15} Hz [5].

1.2.Ferroelectrics

The first ferroelectric material (Rochelle salt) was discovered by Valasek in 1921. Most ferroelectric materials are dielectric materials which show spontaneous polarization even when electric field is not present. This phenomenon is called ferroelectricity.In this case, the positive and negative charges do not coincide with each other even without the electric field thus creates the non-zero value of dipole moment. Ferroelectric materials are majorly used in high dielectric constant capacitors such as multilayer ceramic capacitors (MLCCs), piezoelectric, and biomedical sensors **[6].**

Ferroelectric materials may be classified into two types:

Relaxor ferroelectrics: These ferroelectrics show a wide transformation of phase from the paraelectric to ferroelectric form. They have weak remanent polarization. Relaxor ferroelectrics materials are used as capacitor materials. Near the Curie temperature, they show high dielectric constant and capacitance. The materials like $BaTiO_3$(BT), $K_{1/2}Bi_{1/2}TiO_3$-$BaTiO_3$, $Pb(Mg_{1/2}Nb_{2/3})O_3$ etc. show relaxor behaviour.

Normal ferroelectrics: These ferroelectrics exhibit first or second order transition at Curie temperature (T_c) and follow Curie-Weiss law. Curie temperature vary with change in the frequency. At Curie temperature, they do not show any hysteresis loop. Remanent polarization is large in case of the normal ferroelectric as compared to relaxor ferroelectrics.

1.3 Classification of Ferroelectrics

The ferroelectrics ceramics may be categorized into main four structural types: [7].

(1) Perovskites like $BaTiO_3$, $KNbO_3$, and $Bi_{0.5}Na_{0.5}TiO_3$

(2) Pyrochlore like $Cd_2Nb_2O_7$

(3) Tungsten bronze like $PbNb_2O_6$

(4) Bismuth layer-type compounds like $Bi_{4.5}Na_{0.5}Ti_4O_{15}$

1.3.1 Ferroelectrics with Perovskite Structure

The first perovskite structure was discovered by Gustav Rose in 1839 in Ural Mountains of Russia and it was named after the name of Russian Mineralogist C.L.A. Von Perovski. The general formula of Perovskites is ABX_3 where A and B represent the two cations of unequal

sizes and X bonded to both is an anion. Here, the A-site is occupied by thecationslike Ca^{2+},$Ba^{2+}$and Sr^{2+} and these cations are larger than thecations which occupy the B-site like $Ti^{4+}$and Sn^{4+}) and oxygen atoms is represented by O^{2-}. The A site cation is located at corner position (0, 0, 0). The tetravalent B cations occupy the body centre position (½, ½, ½). Every corner atom is shared by eight another corner atoms while the centre atom is shared by two cubes. The oxygen atoms are located at the face centre of the cubic lattice at position (½, ½, 0) **[8].**

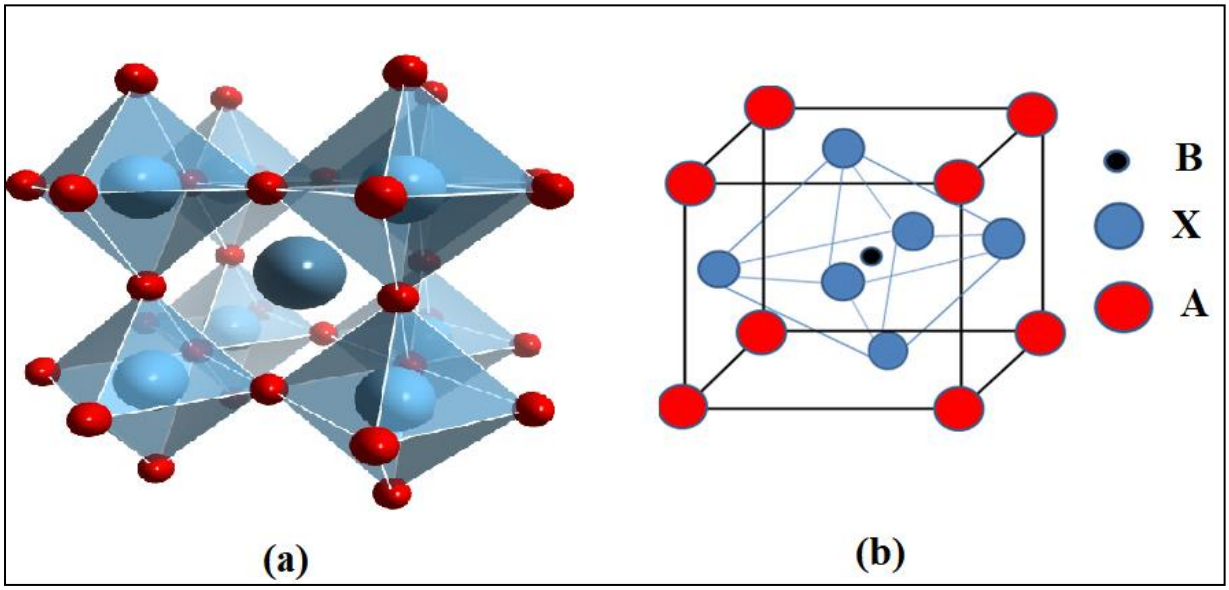

Figure1.2:(a) Three-dimensional network of perovskite structure and (b) Representation of ABX_3 perovskite unit cell [9-10]

Figure 1.2 (a) shows the three-dimensional network of perovskite structure and (b) shows the perovskite structure of a cubic unit cell. The A sites atom has 12 fold coordination numbers, B sites atom has 6 fold coordination number, and the X sites atom is coordinated by 6-fold symmetry. The perovskite structure is mainly an arrangement of BO_6 octahedral where each B-O-B angle is 180º. [11-12]

1.3.2 Ferroelectrics with Bismuth Layer Structure

The family of ferroelectrics which have bismuth layered-structure (BLSFs) was firstly studied by Aurivillius in 1949 [13]. BLSFs have a chemical formula $(Bi_2O_3)^{2+}$ $(A_{m-1}\ B_{\ m}\ O_{3m+1})^{2-}$ where, m is (m = 1, 2, 3, 4, 5), which consists of pseudo-perovskite layers. In this Aurivillius formula, A can be mono-valent, di-valent or tri-valent cation (e.g., Na^+, K^+, Ba^{2+}, Pb^{2+}, or Bi^{3+}), and B

belonging to transition element series (e.g. Ti^{4+}, Nb^{+5}, or W^{6+}) is tetravalent, pentavalent or hexavalent cation. Some examples of bismuth-layered structured ferroelectrics are Bi_2WO_6 (m= 1), $SrBi_2Ti_2O_9$ (m = 2), $Bi_4Ti_3O_{12}$ (m = 3), $Na_{0.5}Bi_{4.5}Ti_4O_{15}$ (m = 4), $Ba_2Bi_4Ti_5O_{18}$ (m = 5) etc.

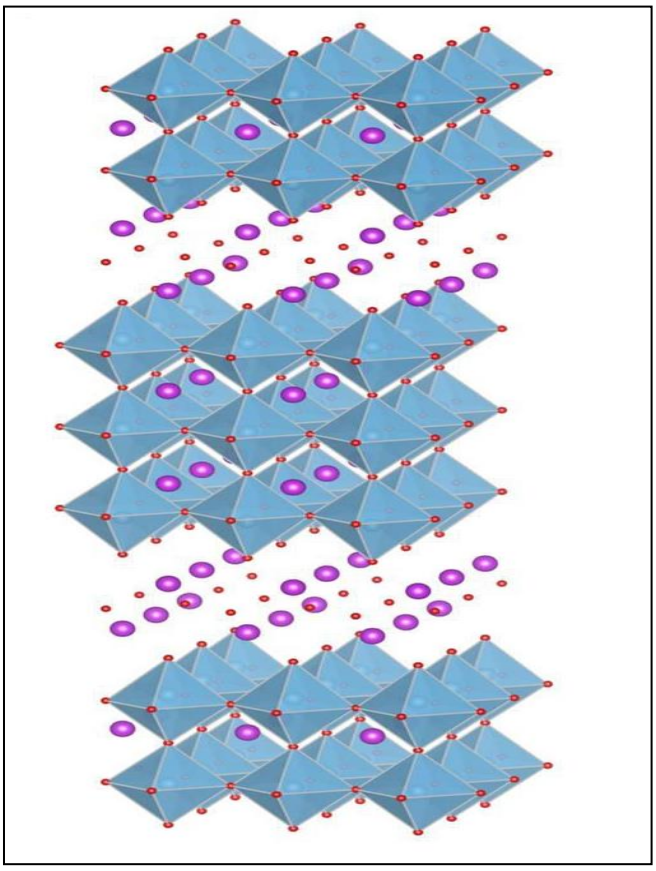

Figure1.3: Bismuth-layered structure

$(A_{m-1}\ B_{\ m}\ O_{3m+1})^{2-}$ perovskites are sandwiched between the $(Bi_2O_3)^{2+}$layers. BLSFs possess tremendous dielectric, piezoelectric, pyroelectric and ferroelectric properties. Bismuth layer-structured ferroelectrics (BLSFs) areincluded in lead-free ceramics which are widely used in potential applications like high-temperature piezoelectric equipment and non-volatile ferroelectric random access memory devices. Figure 1.3 represents the typical structure ofbismuth layered ferroelectrics [7].

1.3.3 Ferroelectrics with Tungsten Bronze Structure

The first tungsten bronze type structure was the lead niobate ($PbNb_2O_6$). It shows interesting ferroelectric properties [14].Till now, hundreds of ferroelectric materials having tungsten bronze structure are enlisted. Figure 1.4 shows the tetragonal tungsten bronze type structure [15].The

general occupancy formula of tetragonal tungsten bronze (TTB) structure is $((A1)_2(A2)_4(C)_4(B1)_2(B2)_8O_{30})$.The TTB structure in perovskite unit cell, corner-sharing BO_6 octahedra, generates three types of sites in a structure: two A-sites are different and one C-site. There are 12-coordinated two A1 sites specified 8 octahedral, 15-coordinated larger four A2 sites specified by 10 octahedral and9-coordinated four trigonal C-sites specified by six (6) octahedra.

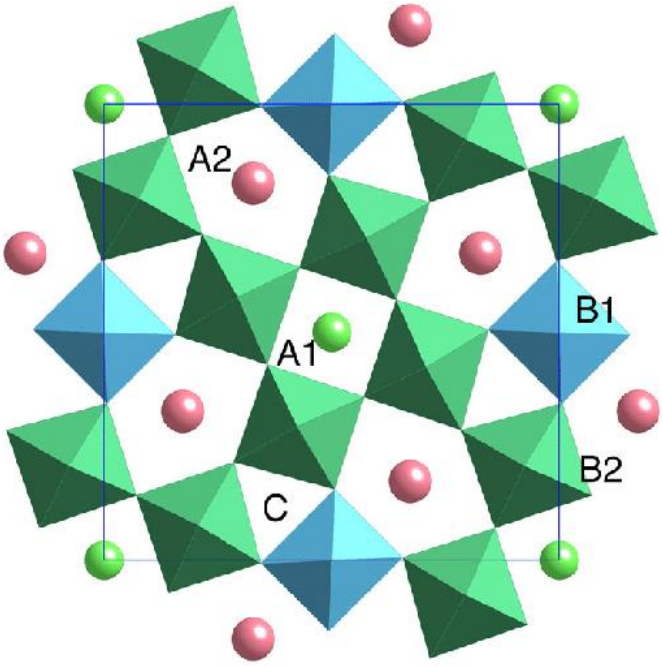

Figure 1.4: Representation of Tetragonal tungsten bronze crystal structure [15]

1.3.4 Ferroelectrics with Pyrochlore Structure

The pyrochlore structure of the materials is represented by the general formula $A_2B_2O_7$, where A represents adivalent or trivalent cation where as B is a tetra- or pentavalent cation. In Figure 1.5 one octant part of pyrochlore is shown in which A^{3+} ions are shown by blue spheres, B^{4+} ions byyellow spheres, and O^{2-} ions by red spheres, respectively. Ferroelectric materials, such as $Cd_2Nb_2O_7$ and $Nd_2Ti_2O_7$ exhibit pseudo-pyrochlore structure. Pyrochlore compounds show interesting properties which are useful for sensors, catalysts, dielectrics and materials [16].

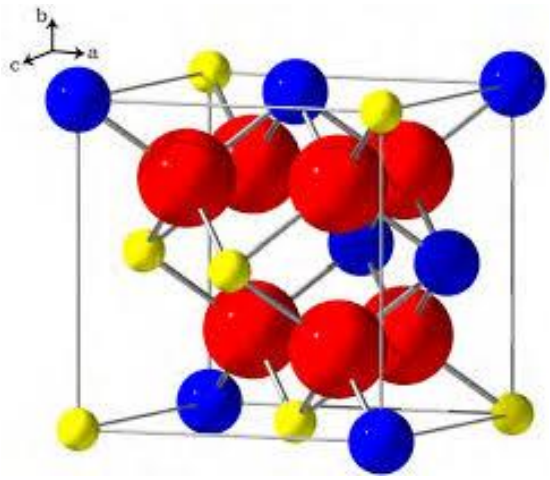

Figure1.5: Representation of pyrochlore structure [16].

1.4 Interrelation between Perovskite and Aurivillus Structure

The constant intergrowth of perovskite $(A_{m-1}\ B_{\ m}\ O_{3m+1})^{2-}$ and $(Bi_2O_3)^{2+}$ fluorite-like layers is described by Aurivillus compound. In the formula 'm' tells the no. of perovskite type units sandwiched between bismuthyl layers. The BO_6 octahedra layers associated with their vertices are a sign of interrealation of bismuth-layer structure and perovskite structure. In NBT-BT structure the concentration is greater than 65 mol% of BT and NBT's concentration greater than 50% the formation of the perovskite structure takes place. At lower concentration Aurivillius phase exist [17].

1.5. Bismuth Sodium Titanate ($Bi_{0.5}\ Na_{0.5}\ TiO_3$)

Among all the lead-free materials, perovskite (BNT) has gained more attention due to its superior ferroelectric properties. Bismuth Sodium Titanate (BNT) was discovered in 1961 by Smolenskii and his co-workers. It is a distorted ABO_3 perovskite structure along with a rhombohedral phase at optimum room temperature [18].BNT exhibits strong ferroelectricity due to high (Curie temperature) (T_c = 320 ℃), remanent polarization (P_r =38μC/cm^2), and with a large coercive field (E_c=73 kV/cm) [19].

1.5.1. Crystal structure

The distorted ABO_3 structure of BNTcan be demonstrated by two different ways: one way is sodium and bismuth occupy the corner position in a unit cell, titanium cation occupies the position in the centre, and oxygen cations occupy at face centres which form octahedra. Another way is three-dimensional arrangements of 8-corners occupied by TiO_6 octahedra with bismuth nd

sodium cations are at the centre position in the unit cell. Figure 1.9 shows the cubic unit cell structure of BNT.

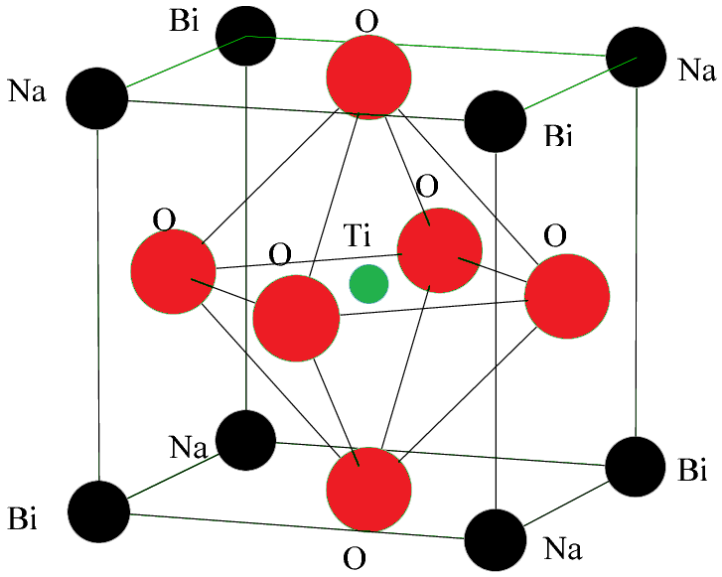

Figure 1.6: Sodium Bismuth Titanate (BNT) crystal structure [20]

1.5.2 Phase transition in BNT

Two-phase transformation is observed in this material. BNT undergoes the following transformation from cubic phase to tetragonal to a rhombohedral phase when mixed with compounds such as barium titanate (BT), potassium sodium niobate (KNN) etc. of perovskite-ferroelectric phase structure. The transformation from cubic to tetragonal corresponds as paraelectric to anti-ferroelectric phase and tetragonal to rhombohedral corresponds as anti-ferroelectric to ferroelectric with varying temperature. Yet, the two other characteristic transition temperatures T_d and $T_m$were obtained is known to be depolarization temperature and maximum dielectric constant temperature. It shows high dielectric constant and high tangent loss at low temperatures [21-22]. BNT is polar in the rhombohedral phase and it behaves as relaxor ferroelectric in this phase.

Besides all the good ferroelectric properties, it has some issues like high dielectric loss, high coercive field, high conductivity. The main limitation of high conductivity is due to volatilization of Bi^{3+} ions during the sintering process. Although several studies on NBT based systems with various substitutions, solid solutions of NBT exhibit improved properties. These systems near

their MPB exhibit piezoelectric, ferroelectric and electromechanical properties comparable with the Pb-based ferroelectric materials.

CHAPTER 2

LITERATURE SURVEY

The primary aim of the present study is to synthesize BNT and BT-doped ceramics. For this purpose, a detailed literature survey on synthesis of Bismuth Sodium Titanate (BNT) has been done. The important key findings investigated by different research groups have been discussed and outlined in the chronological order:

2.1 Literature Survey

Chu *et al.* **in 2002 [23]** examined the morphotropic phase boundary of lead-free piezoelectric (1-x)$Na_{0.5}Bi_{0.5}TiO_3$-x$BaTiO_3$(x = 0.1, 0.08, 0.06, 0.04, 0.02) ceramics near (x=0.06). X-ray data confirmed the rhombohedral-tetragonal MPB exists in this compound.With the increasing composition of (0.08, 0.1) the rhombohedral phase turned into tetragonal phase. From these results found that the (T_m) maximum temperature is higher than depolarization temperature(T_d). These ceramics possess the properties of low dielectric permittivity, high frequency, and thus, can be used for ultrasonic applications.

Li *et al.* **in 2004 [24]** investigated the effects of Nb^{5+}, Co^{3+}, or La^{3+}substitution on BNBT-6 system by studying the dielectric, piezoelectric, and microstructural properties. It was observed that with the doping of Nb^{5+} and La^{3+}, there is a change in dielectric constant near 100℃ , after that peak begins to broaden. That indicate the intermediate phase transition. The intermediate phase transition disappears with doping Co^{3+}. microstructural analysis showed that all compounds of Co^{3+} doped BNBT6 have larger grain size than Nb^{3+} and La^{3+}.

Guo *et al.* **in 2004 [25]** prepared the ($Na_{0.5}K_{0.5}$) NbO_3-$BaTiO_3$ by a Mixed-oxide route method. The addition of $BaTiO_3$ in KNN increase the grain size and it completely diffuses into KNN to form solid-solution. XRD analysis revealed that phase changes from orthorhombic to tetragonal at x = 0.06, and tetragonal to cubic at x= 0.20. At low concentration of BT, it showed good piezoelectric and ferroelectric properties with (P_r =7.5 μC/cm^2, E_c=12kV/cm,ε_r = 1003, tanδ = 3.8%, T_c= 358 ℃, d_{33} =104pC/N).

Sanson *et al.***in 2005 [17]**studied the $Na_{0.5}Bi_{0.5}TiO_3$-$Bi_4Ti_3O_{12}$-$BaTiO_3$ compounds. They reported the Aurivillus structure present by XRD analysis below 20°. At higher angles it shows perovskite structure. XRD results showed that at greater than 65 mol% of BT and NBTgreater than 50% the perovskite structure appeared. At lower concentration Aurivillius phase exist.

Wang *et al.* **in 2008 [26]**investigated that piezoelectric properties of cobalt-modified NBT ceramics were enhanced. The incorporation of Co into NBT improved the piezoelectric ceramics which leads to Curie temperature T_c (663 ℃) and piezoelectric constant d_{33} (30 pC/N).

Zhao *et al.* **in 2008** [**27**] prepared $Na_{0.5}Bi_{4.5}Ti_4O_{15}$-(x-1)$Na_{0.5}Bi_{0.5}TiO_3$composite ceramics. Over the composition range upto (x = 2 - 99), the coexistence of perovskite and layered bismuth-structure phase was confirmed by XRD technique. The two dielectric behaviour 350℃ and 670℃ of this composite ceramics in this range also confirmed the coexistence of two phases. SEM studies showed plate-like grains with small cubic shape grains indicating the bismuth-layered structure and perovskite structure.

Wang *et al.* **in 2009 [28]** investigated thedielectric, ferroelectric, piezoelectric, and electromechanical properties of NBT-Li, Ce ceramics. They reported that piezoelectric properties enhance with the addition of Li, Ce. Because of high Curie temperature (T_c= 660°C), these ceramic are used for high-temperature applications.

Rout *et al.* in **2009 [29]** reported that the presence of rhombohedral-tetragonal morphotropic phase boundary in (100-x)$Na_{1/2}Bi_{1/2}TiO_3$-x$BaTiO_3$solid solution ceramics with varying the composition ($0 \leq x \leq 10$). It was observed that the MPB lies in the system at composition of $(x = 5.5)$. The splitting into two peak at 5.5 is completely show the phase trnformed from rhombohedral into tetragonal. Itwas also confirmed by Raman spectroscopy.

Cernea *et al.* **in 2009 [30]** prepared the BNT-BT0.08 ceramics by sol-gel method.These ceramics were sintered at 1100ºC and 1150ºC. Dielectric properties (ε_r = ~4500 and tanδ = ~ 0.03) and high (Q_m~ 500) were observed from these results.

Ahn *et al.* **in 2010 [31]** studied the $Na_{0.5}Bi_{4.5-x}La_xTi_4O_{15}$ (NBLT) and $Na_{0.5}Bi_{4.5-x}Nd_xTi_4O_{15}$ (NBNT) lead-free bismuth layered structure. In the (NBLT) and (NBNT) ceramics with increasing the concentration the Nd and La, the Curie temperature and permittivity was decreased but broadened the dielectric constant curve.

Gao *et al.* **in 2011 [32]** prepared $Na_{0.5}Bi_{4.5}Ti_4O_{15}$+ 0.375 wt% $MnCO_3$ lead-free piezoelectric ceramics. These results signify that with the $MnCO_3$ addition, the ferroelectric and piezoelectric properties had been increased while dielectric loss get decreased (d_{33} = 28 pC/N, E_r =140, k_p = 0.06, Q_m = ~3290, and tanδ = 0.3 %.). Based on this study, it was found that ceramic has high thermal stability up to 500℃ and it promotes grain growth and densification.

Sun *et al.* **in 2011 [33]** synthesized (1-x)BT-xNBT ceramic by doping of Nb, Co samples via solid- route method with varying concentration of x (0- 0.4). At x = 0.2, the dielectric constant at optimum room temperature was observed to be 2500.

Parija *et al.* **in 2013 [34]** synthesized the (1-x) BNT-xBT ceramic where (x = 0.07, 0.05, 0.03, 0.01) via solid route method and sintered at 1150 ºC for 4 hours. At 0.07, MPB was found between rhombohedral and tetragonal phase, which was confirmed by XRD and Raman spectroscopy analysis. They have studied that the phase transition temperature (T_m) gradually decreases, permitivity and diffusivity increases with rise of Ba content. The dielectric and piezoelectric properties like E_c, P_r increases with an rise of BT content.

Jiang *et al.* **in 2014 [35]**studied the effect of (Nd, Ce) substitution for A-site on NBT -based ceramics. They investigated that $Na_{0.5}Bi_{4.3}$ $(Nd_{0.5}Ce_{0.5})_{0.2}Ti_4O_{15}$ ceramic is a promising material for high-temperature piezoelectric equipment because it has high T_c (630 ℃), high d_{33} (28pC/N), high Q_m (3239). With increased (Nd, Ce) content, the Curie temperature T_c is decreasing from 638℃ to 618℃.

Hussin *et al.* **in 2015 [36]** studied that bismuth layered structure BNT4 ($Na_{0.5}Bi_{4.5}Ti_4O_{15}$) transformed into a single phase perovskite structure through a topo-chemical conversion process using reactants Na_2CO_3 and TiO_2 at 950 ℃ for 4 h. The BNT templates result showed the formation of pseudo-cubic structure, relaxor behaviour, good ferroelectric response at (E= 90Kv/cm, P_r = 32 μC/cm^2, E_c=56 kV/cm.)

Jiang *et al.* **in 2016 [37]**synthesized the(NBT-KNN-100x) where (x = 0.15, 0.10, 0.05 and 0.00) ferroelectric ceramics. Ferroelectric properties were improved by addition of KNN with permitivity increase upto 24pC/N. They concluded that as KNN increases with weak strucrural distortion of TiO_6 octahedral show lower Curie temperature.

Shamim *et al.* **in 2017 [38]** prepared the lead-free $(Na_{0.47}K_{0.47}Li_{0.06})$ NbO_3 ceramics by microwave sintering method at 1050 ºC and 1150 ºC and their structural, dielectrical and electrical properties were measured. The existence of orthorhombic symmetry with a minor

secondary impurity phase of tungsten bronze structure was confirmed byXRD analysis.These results informed that Curie temperature shift to the lower side then they increase the dielectric permittivity and decrease the tangent loss. A non-Debye relaxation nature is observed for the sample.

Zhang *et al.* **in 2017 [39]** prepared $Na_{0.5}Bi_{4.5}Ti_4Mg_xO_{15+x}$ and $Na_{0.5}Bi_{4.5}Ti_{4-x}Mg_xO_{15-x}$ ceramics (x = 0.04, 0.08), shows that a single phase formation of bismuth layer-structured ferroelectrics. All the dielectric and ferroelectric properties enhanced with the variation in Mg content. These results inform that Curie temperature Tc (660℃) is high for all the samples. In this ceramics, a wide temperature range with high permitivity and low tangent loss was obtained that is useful in the application of high-temperature capacitors.

Sahoo *et al.* **in 2017 [40]** examined the BNT ceramic with the addition of (8 wt %) barium titanate (BT) by mixed-oxide method, shows the two-phase formation orthorhombic (major) and tetragonal (minor) phase at room temperature. Less porosity, high density and grain growth were observed by SEM technique.The dielectric constant increase and tangent loss decrease, with the small substitution of BT in BNT ceramic that is suitable for many devices. A non-Debye relaxation phenomenon is observed by dielectric and impedance spectroscopy. The results revealed that activation energy is also calculated at the different frequency by electrical conductivity.

Liu *et al.* **in 2018 [41]** examined the effect of MgO doping on the $Na_{0.5}Bi_{0.5}TiO_3$-$BaTiO_3$ ceramic and their structural, ferroelectric, and dielectric properties. As the doping content of MgO is 0.5% , it shows good ferroelectric properties with (P_r = 52.57 μC/cm^{-2}). If doping amount is 1.5% or above, it depicts large permittivity and low tangent loss with strong relaxation.

Hajra *et al.* **in 2018 [42]** prepared the BNT-BT-4 ceramic using the conventionally solid-state reaction method.The results showed that the homogenous distribution of grains with high-density formed in the sample. They observed that with rising temperature; decrease the size of grain show a negative temperature coefficient of the material.

Munir *et al.* **in 2018 [43]** synthesized the $0.965Bi_{0.5}Na_{0.5}TiO_3$-$0.035BaTiO_3$ (BNT-BT) ceramics using sol-gel technique and powder were Calcined at 600 ºC. By XRD analysis pure perovskite structure of BNT-BT samples is observed. The P_r is 34.8μC/cm^2 with a E_c of 23kV/cm obtained at sintering temperature 1150ºC. The high piezoelectric constant (d_{33}=138 pC/N) was also measured at 1150ºC temperature.

Jiang *et al.* **in 2019 [44]** reported that ferroelectric and piezoelectric properties of $Na_{0.5}Bi_{4.5}Ti_4O_{15}$-BT ceramics improved by the addition of Mg using solid-state reaction method and were sintered at 1040 ℃. They examined that the piezoelectric coefficient (d_{33}) is 20pC/N and maximum ($2P_r$) is 3.08μC/cm^2 with a field (E_c) of 18.01kV/cm. Moreover, permittivity and tangent loss were found to be 486 and 0.17 at frequency 10kHz.They optimized that with Mg doping enhance the electrical-BT composite properties which imply that it has a great range of applications in electronic devices.

Munir *et al.* **in 2019 [45]** prepared the $Bi_{0.5}Na_{0.5}TiO_3$ nanopowders by using the sol-gel technique and were sintered at different temperatures (950 ºC – 1150 ºC). This result shows that P-E loops at these (950 ºC and 1000 ºC) are leaky. But it enhanced with above 1050 ºC sintering temperature.

Turki *et al.* **in 2019 [46]** investigated the $(Na_{0.5}Bi_{0.5})_{0.94}$ $Ba_{0.06}TiO_3$ (NBT-6BT) ceramic with the doping of Sm, by conventionally mixed route method. The doping of Sm in lower amount (≤8mol. %) signify the presence of two of tetragonal and rhombohedral structures,while with a higher composition of Sm (11mol. %) show pseudo-cubic structure.The temperature dependence of dielectric permittivity indicates that the change of phase from ferroelectric to anti-ferroelectric at low temperature, after that to paraelectric phase at higher temperatures. It was found that the dielectric measurement exhibit relaxor behaviour at transition 'T_d', 'T_m' . With the small amount of Sm doping, it improves the dielectric permittivity, ferroelectric and piezoelectric properties. (P_r =31μC/cm^2,d_{33} = 140pC/mm, k_p =0.28 and k_t =0.18.)

Based on the literature survey, it is evident that $Na_{0.5}Bi_{0.5}TiO_3$ exhibit rhombohedral phase and $BaTiO_3$ exhibit tetragonal at room temperature. When the concentration of BT is increased in BNT is then the system depicts mixed phase ofperovskite and Aurivillus structure. The different parameters together with synthesis method, Curie temperature, dielectric constant, Morphotropic phase boundary are summarised in Table 2.1.

Table 2.1 Properties of various compounds

S. No.	Compound	Synthesis method	ε_r	tanδ	T_d °C	T_C °C	d_{33} pC/N	P_r μC/cm^2	E_c kV/ cm
1.	(1-x) BNT-xBT (x = 0.01, 0.03, 0.05, 0.07) [34]	Solid-state reaction method	4773	0.01	165	-	134	16.4	16.8
2.	NBT-BT-xMgO (x = 0, 0.5, 1, 1.5, 2) [41]	Solid-state reaction method	-	-	-	-	164	41.0	39.2
3.	0.965BNT-0.035BT [43]	Sol-gel technique	-	-	-	-	138	34.8	23
4.	(1- x)BT-xNBT (x = 0.02, 0.04, 0.06, 0.08,0.1) [23].	Conventionally mixed-oxide method	601	0.017	100	-	122	40	-
5.	$Na_{0.5}Bi_{4.5}Ti_4O_{15}$+ 0.375 $MnCO_3$ [32]	Conventionally Solid-state method	140	0.3	3290	500	28	-	-
6.	NBT-Co doped [26]	Mixed-oxide route	152	0.10	-	663	30	-	-
7.	$Na_{0.5}Bi_{4.5}$ Ti_4O_{15}-BT [44]	Conventionally mixed-oxide route	486	0.17	-	543	20	3.08	18.0

CHAPTER 3

Materials and Methods

3.1.Materials

BNT(Sodium bismuth titanate) and BT (Barium Tiatanate)-BNT (Sodium bismuth titanate) samples were synthesized using solid-state reaction method.

$(1-x)(Bi_{0.5}Na_{0.5})TiO_3$-$xBaTiO_3$ (x = 0, 0.1, 0.2, and 0.3) (abbreviated as BNT-BT0, BNT-BT10, BNT-BT20, BNT-BT30) samples were synthesized and have been characterized for their crystallographic structure, morphological, compositional,dielectric and ferroelectric properties.

3.2. Synthesis of BNT and doped BNT ceramics

The BNT ceramics are synthesized via conventional solid-state reaction method. This method is performed through mixing two or more compounds. The ingredients consist of oxides and carbonates which were bismuth oxide, sodium carbonate, barium carbonate and titanium oxide. These compounds were weighed based on their stoichiometric formulae. For the preparation of BNT, compound were thoroughly mixed using agate mortar and pestle and ground for 8-10 h in acetone medium to make a homogenous mixture. After the mixing and grinding, the mixture of NBT powder was calcined at 900 ℃ for 3h and sintered at 950 ℃ for 2h. The calcined fine powder was pressed and compact in pellets using polyvinyl alcohol(PVA) as a binder into a disc of diameter 10 mm and thickness 1to 2mm by hydraulic press machine.For the preparation of BT doped NBT ceramics, the same procedure was followed. After the mixing and grinding, we calcined the (1-x) $(Bi_{0.5}Na_{0.5})TiO_3$ -x $BaTiO_3$ powder with composition (x = 0.1, 0.2, 0.3) at the 900 ℃, 1000 ℃, 1000 ℃ temperature for 3h and sintered at 950 ℃ for 2h , (1010 ℃, 1010 ℃) for 3 h, respectively.

3.3.Flow Chart of work:

Flow chart for the preparation of BNT ceramic –

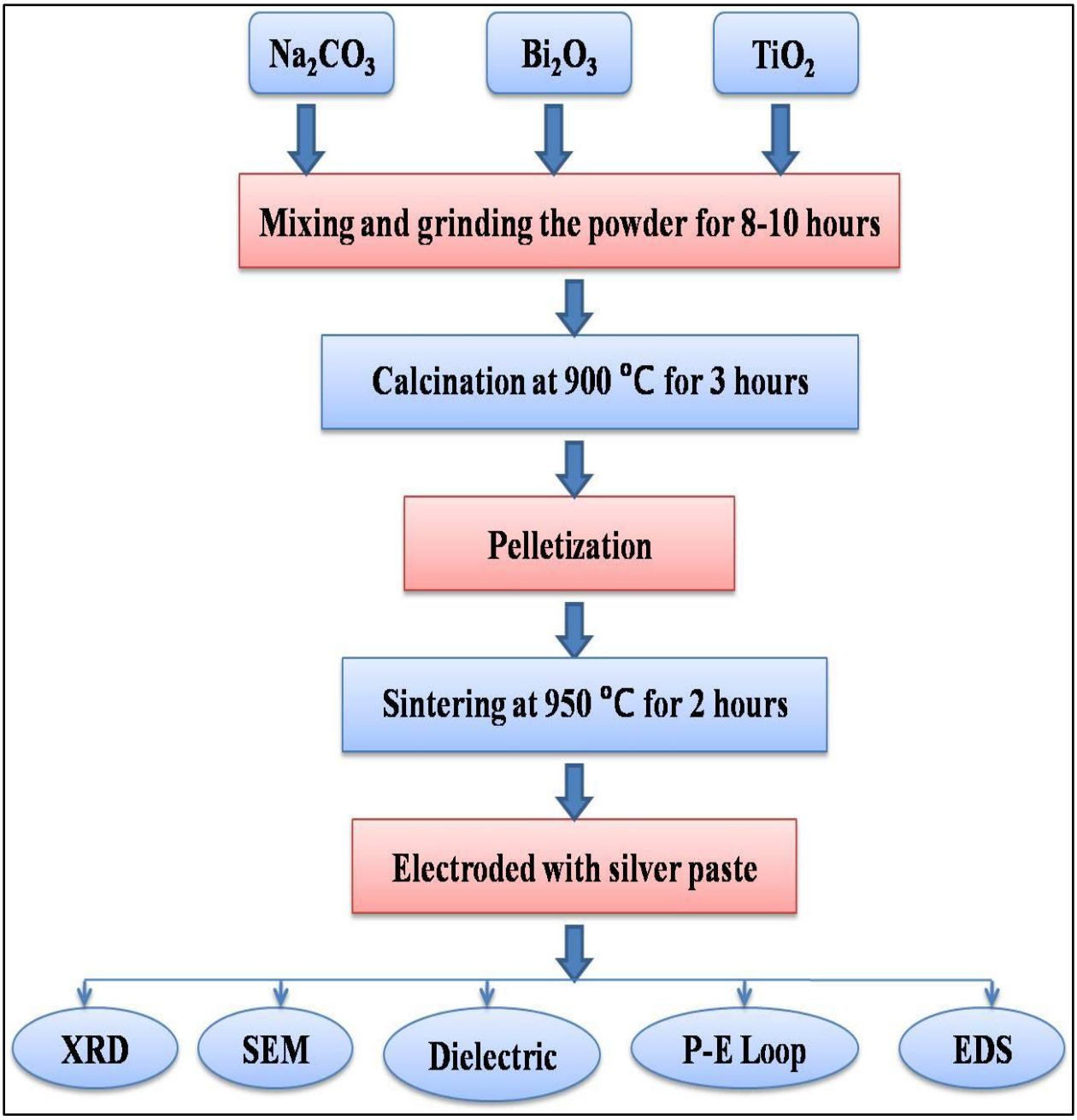

Figure 3.1: Flow chart for BNT powder preparation

Flow chart for the preparation of Ba doped BNT ceramic-

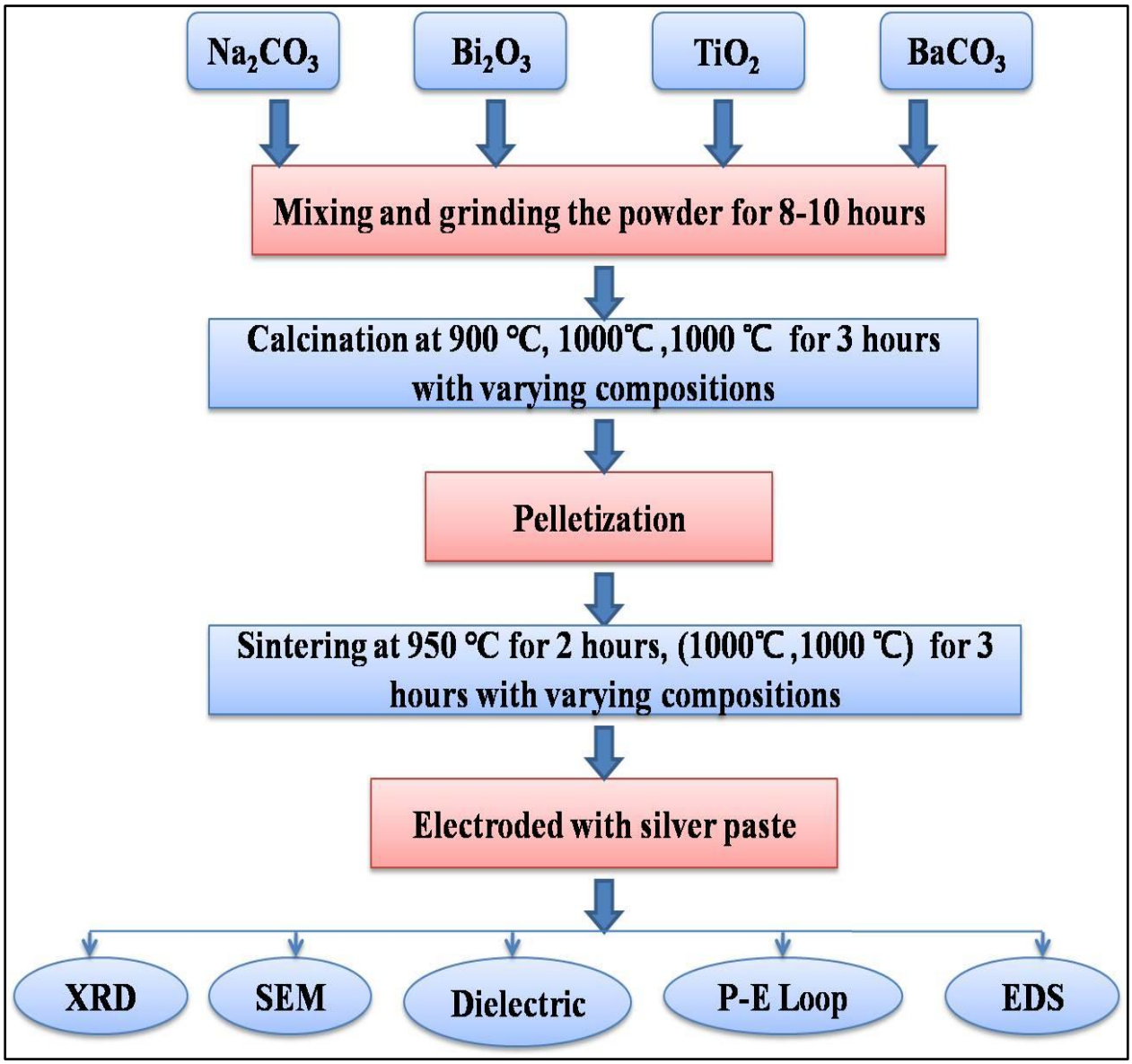

Figure 3.2: Flow chart for Ba doped BNT preparation

3.4 Characterization Techniques

3.4.1 X-ray Diffraction

X-Ray Diffraction broadly helps in structural characterization from which phase identification, crystallite size and lattice constant or unknown crystalline substance can be easily determined. This method is based on determining the scattering intensity of the X-ray beam. The X-rays are

electromagnetic in nature having range between 120eV-120keV. The X-Ray diffraction follows Bragg's law principle.

3.4.1.1 Bragg's law

It is used for examining the structural properties of the materials and arrangement of atoms which satisfies Bragg equation.

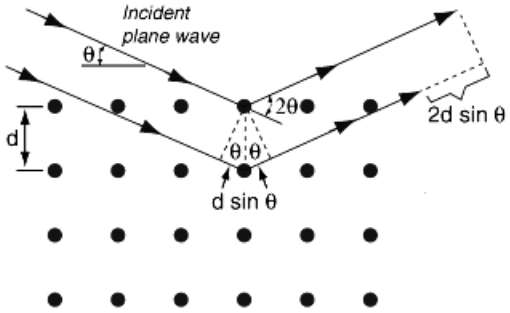

Figure 3.3: Bragg's law of diffraction

The Bragg's equation is given as:

$$2d \sin\theta = n\lambda$$

Where'd' is the inter-planar spacing , n is a positive integer, λ corresponds to wavelength of incident X-Rays and θ corresponds to Bragg's angle.

Figure 3.4: XRD apparatus

The X-Ray diffraction measured by PANalytical's XPERT PRO (SAIF PU) using Cu-Kαradiation($\boldsymbol{\lambda = 1.54}$Å**)** with Ni-filter. The angle of measurements was 20º to 80º in 2θ range at room temperature.

3.4.2. Scanning Electron Microscopy

The scanning electron microscopy is a powerful method to analyze the morphology and topography of synthesized materials providing high resolution. SEM works on the principle where highly energetic beam of electrons are used to bombard the sample using various radiations like x-rays, secondary electrons, ejecting back-scattered electrons from the surface of sample. A High energetic ray of electrons raster scans the surface. The radiations collected by the detector are displayed on a screen after getting converted into signal. It provides information about the shape of grains, grains boundaries, variation in size and porosity of the materials. The samples were coated with an ultrathin layer of gold by a sputtering method. We used JEOLJSM-6510LV model for SEM analysis from SAI Labs TIET Patiala.

Figure 3.5: SEM apparatus

3.4.3 Energy Dispersive Spectroscopy (EDS)

Energy Dispersive Spectroscopy(EDS or EDX) is a useful technology helps to identify the line intensities, chemical composition, and elemental mapping of the materials. It is conjugate with the SEM and it can detect all elements from 4(Be) to 92(U). A highly energetic beam of electrons by SEM is a strike on the sample, the various interactions take place and the radiations like x-rays and secondary electrons. During the ejection of electrons, some vacancies are created at the surface of atom.To fill these vacancies, electrons having high energy jumps to lower energy state with the emission of x-rays. Thus, an atom can be identified by the measuring of the amount of energy released.

Figure 3.6: EDS attached with SEM

3.4.4 Dielectric Measurement

The NumetriQ model PSM 1735 was used for this measurement. LCR meter measure the dielectric permittivity and tangent loss at different frequencies (100Hz-1MHz) with various temperatures ranges (50 ºC - 600 ºC). For the dielectric measurement the conductivity of the pellets were managed by using silver paste. The dielectric constant was calculated by using this formula:

$$C = \varepsilon_0 \varepsilon_r \frac{A}{d}$$

$$\varepsilon_r = \frac{C_P}{C_0}$$

$$C_0 = \varepsilon_0 \frac{A}{t}$$

$$A = \frac{(\pi d^2)}{4}$$

Where A= Area of the pellet (mm^2), t= Thickness of the pellet (m), d = diameter of the pellet (m), ε_o = free space permittivity (8.85 x 10^{-12} F/m), C_P = parallel capacitance, C_o= capacitance in vacuum.

Figure 3.7: Dielectric instruments

The dielectric properties of the material tells us about the material's stability.The nature of the material, like normal or relaxor ferroelectric is confirmed after observing the dielectric data. Dielectric of the material provides information about the impedance of the sample. Real and imaginary components represents the impedance of the sample. The real part of impedance has the ability in order to store electrical energy while the imaginary part is the dissipation factor of the material. Impedance parameters are given as:

$$Z^* = Z' - jZ''$$

$$Z^{"} = \frac{1}{\omega C_S}$$

Where $\omega = 2\pi f$ is the angular frequency, z' is real component and z" is imaginary component of relative permittivity. The plots between z' is on the x-axis and z" is on the -axis is known as Cole-Cole plot.

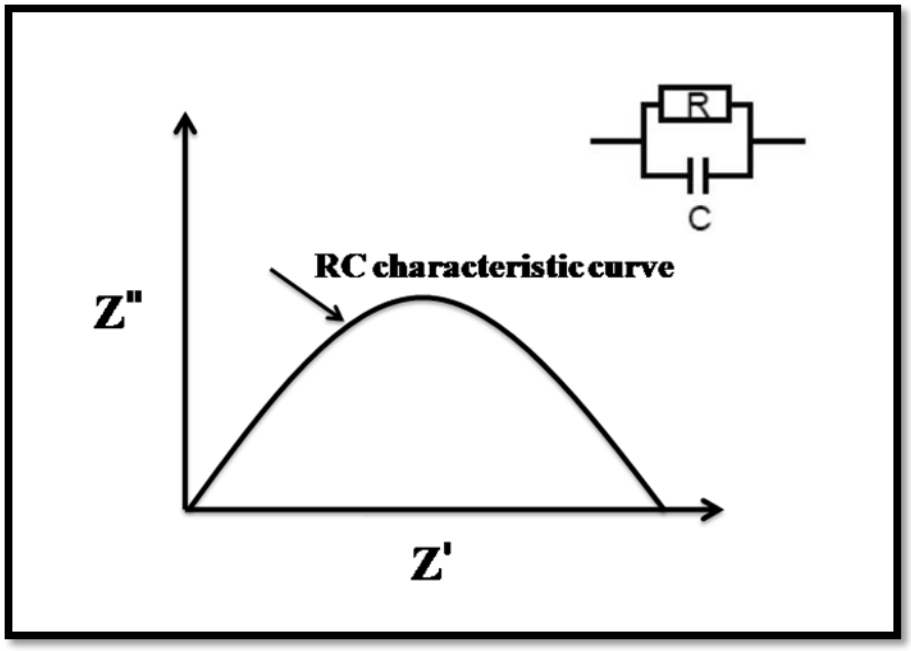

Figure 3.8: Cole-Cole plot

3.4.5 Ferroelectric P-E loop tracer

The ferroelectric property of the substance is confirmed by hysteresis loop. This loop tracer depicts the plot between the polarizations (P) versus applied field (E). The value of electric parameters like spontaneous polarization (P_s), remnant polarization (P_r) and the coercive field (E_c) are determined by studying the hysteresis curve. The basic principle of the P-E loop tracer is depend on the Sawyer-Tower circuit. The Sawyer-tower circuit measures the voltage across the sample. For P-E loop measurement, the sample was placed in silicone oil. The data was collected at optimum room temperature with a voltage applied in a series of steps.

Figure 3.9: P-E loop tracer

Automatic PE Loop Tracer by MARINE INDIA was used for ferroelectric studies.

CHAPTER 4

RESULTS AND DISCUSSIONS

4.1. X-ray diffraction (XRD)

The XRD spectra of BNT-BT0, BNT-BT10, BNT-BT20, and BNT-BT30 are shown in Figure 4.1. The peaks were matched and indexed with the standard ICDD cards (ICDD card No.00-036-0340), which provided information about the phases occuring in the compounds. The preliminary structural analysis of this pattern suggests that the compound has a major $Na_{0.5}Bi_{0.5}Ti_4O_3$perovskite phase with a small peak near 30º corresponding to $Na_{0.5}Ti_4Bi_{4.5}O_{15}$(Aurivillus phase)phase. It is usually formed along with $Na_{0.5}Bi_{0.5}Ti_4O_3$ at the time of heating at higher-temperature **[40].**Though there is a mixture of two phases in the sample viz rhombohedral and tetragonal, the amount of the tetragonal phases is lesser than that of the rhombohedral phases. It is observed that with increasing the composition of $BaTiO_3$, the rhombohedral phase may be transformed into Aurivillus phase. At higher concentration, we observed that many peaks of aurivillus phase(i.e. marked by ♦)appeared. A peak of Barium titanate (ICDD card No.00-042-0457)occurred near 28º for BNT-BT20 and BNT-BT30 (marked by *****). Secondary tetragonal phase is because of solubility gap, differences in the composition and metastable coexistance [40].Simliar results have been reported by Zhao et al. [27].

The calculated lattice parameters (hexagonal equivalent) are a=b=5.47 Å, c=6.69 Å for BNT-BT0, a=b=5.48 Å, c=6.75 Å for BNT-BT10, a=b=5.48 Å, c=6.68 Å for BNT-BT20 and a=b=5.5 Å, c=6.79 Å for BNT-BT30. From 4.2 it is clear that diffraction peaks shift to lower 2θ angles with doping of Barium Titanate because the ionic radius of Ba^{2+}(1.42 Å) is greater than that of both Bi^{3+} and Na^{+} (1.17 Åand 1.18 Å respectively), which distorts the lattice. **[29].**

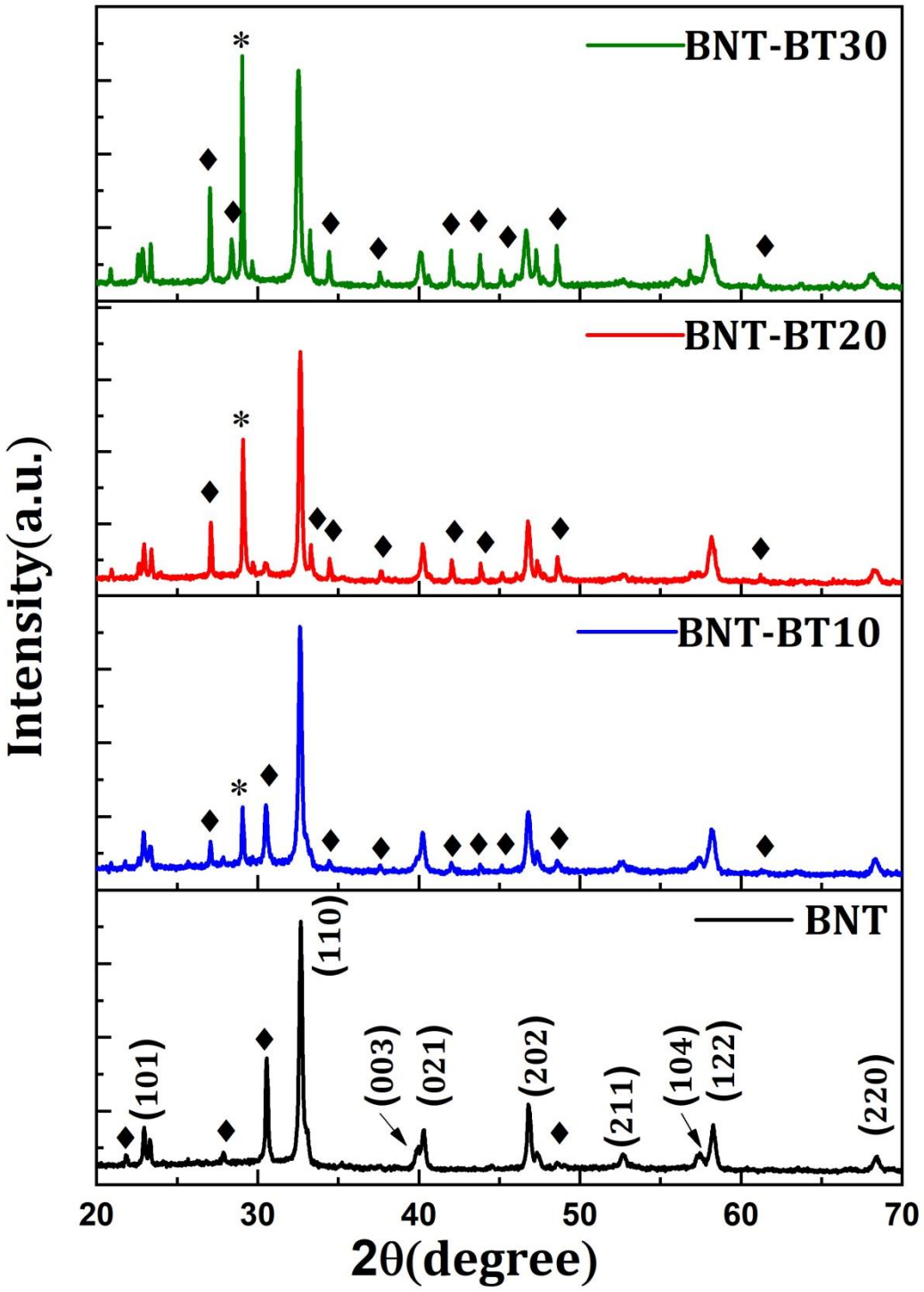

Figure 4.1 XRD patterns of the BNT-BT0, BNT-BT10, BNT-BT20, and BNT-BT30 ceramics

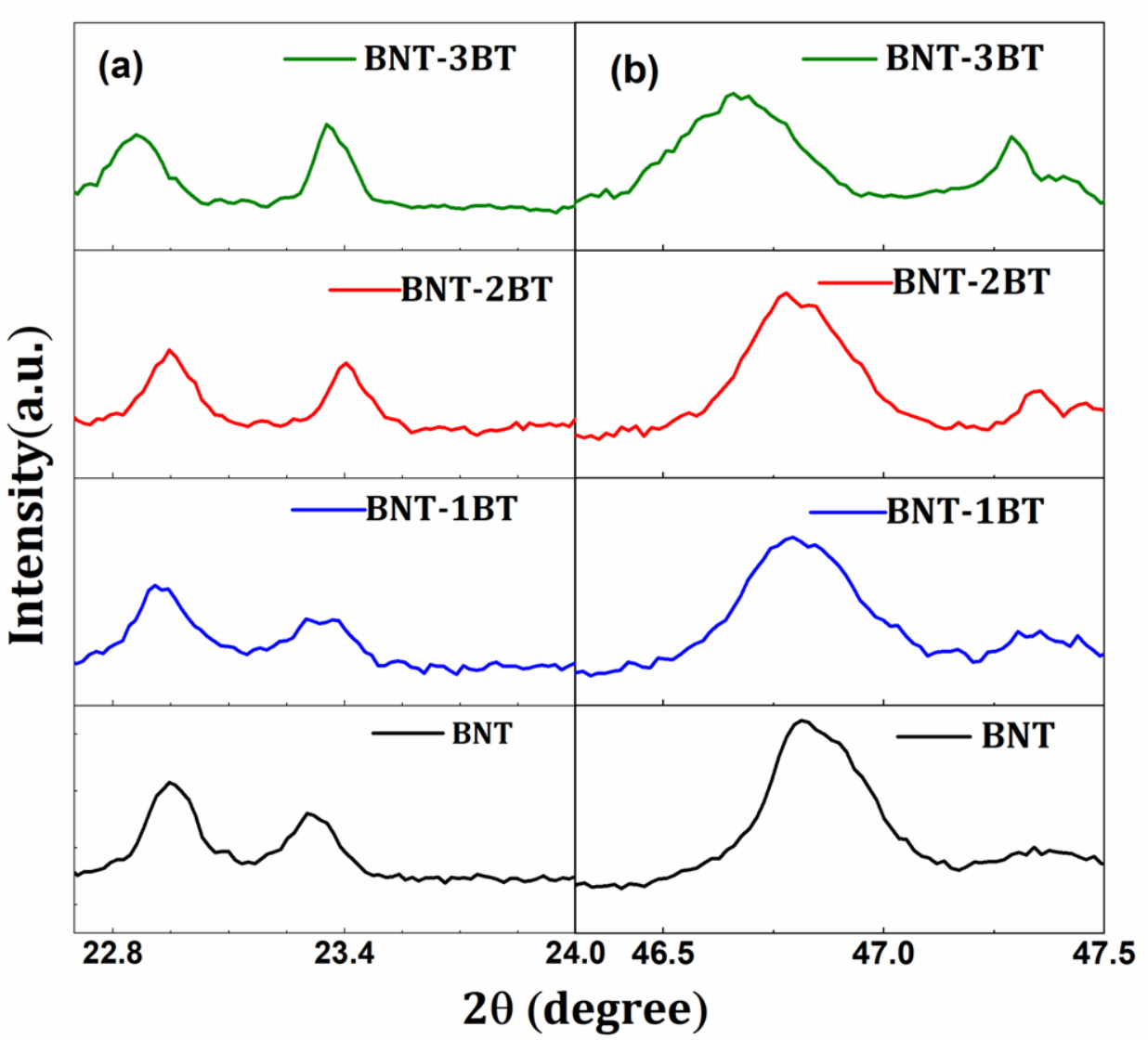

Figure 4.2 Zoomed XRD patterns of BNT-BT0, BNT-BT10, BNT-BT20, and BNT-BT30 ceramics

4.2. SEM and EDS Analysis

The microstructure and morphological features of samples were analyzed using a scanning electron microscope. Figure 4.3 shows the SEM and EDS photographs of the sintered sample which is taken at a magnification of 20000. The SEM micrograph shows, there is a non-uniform distribution of grains with dense microstructure. Energy dispersive spectroscopy (EDS or EDX) is used to examine the chemical composition of the sample. All the elements (O, Ti, Bi, Ba, Na) are distributed homogeneously.

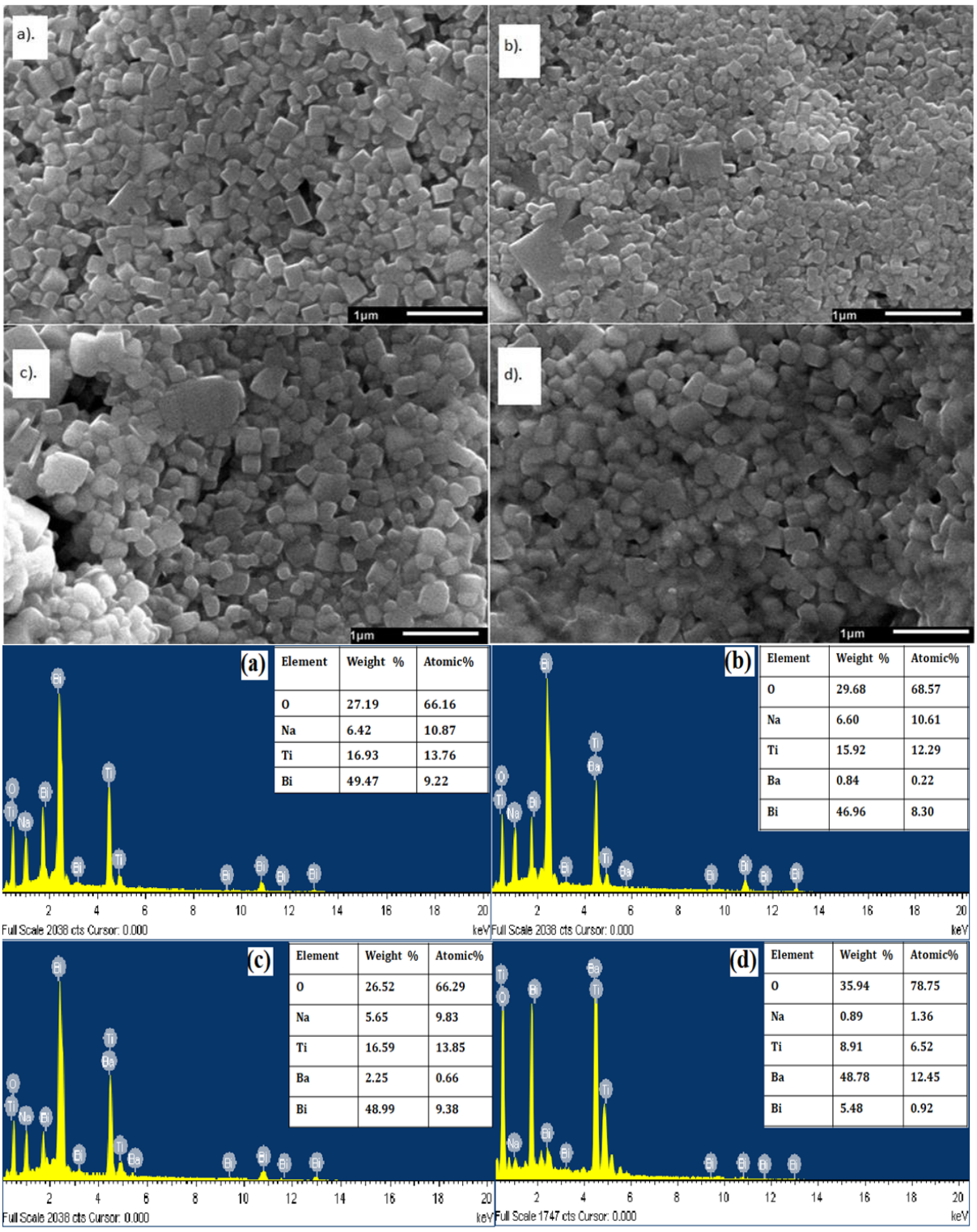

Figure 4.3: Microstructure and EDS (spectra or table) of (a) BNT-BT0, (b) BNT-BT10, (c) BNT-BT20, and (d) BNT-BT30 ceramics at magnification of 20000.

4.3.Dielectric measurements

Figure 4.4 (a-h) depicts the variation of dielectric constant and dielectric loss with temperature for BNT and doped BNT ceramics ranging from room temperature to 500 ℃ at frequencies of 1 MHz, 100 kHz, 10 kHz, 1 kHz, and 100 Hz respectively. They show a broad diffuse peak at Curie temperature at all the frequencies for all the compositions. This could be attributed to the relaxor behaviour. **[49].** The dielectric constant is found to decrease with increase in frequency. With increasing the Ba^{2+} amount, dielectric constant increase except for 0.1 composition due to space charge polarization.

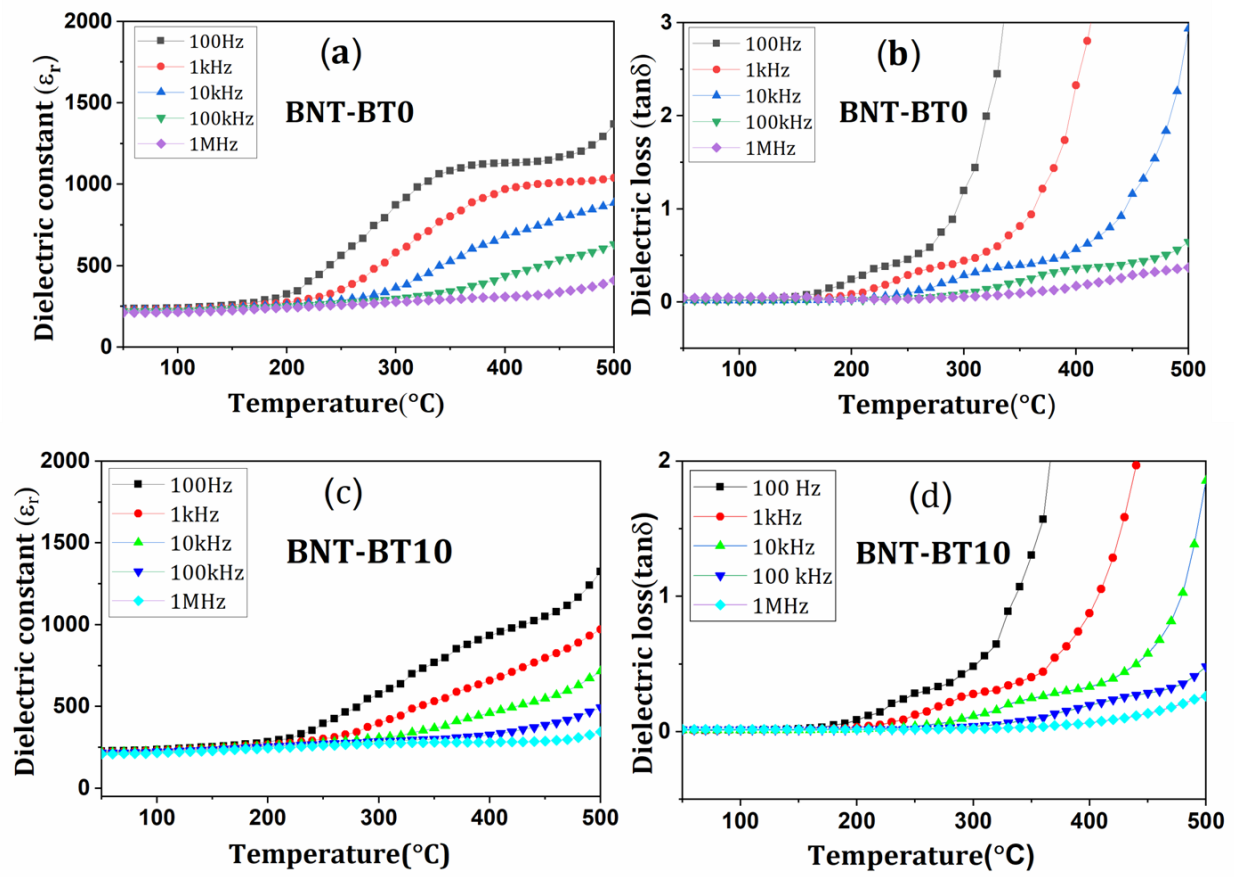

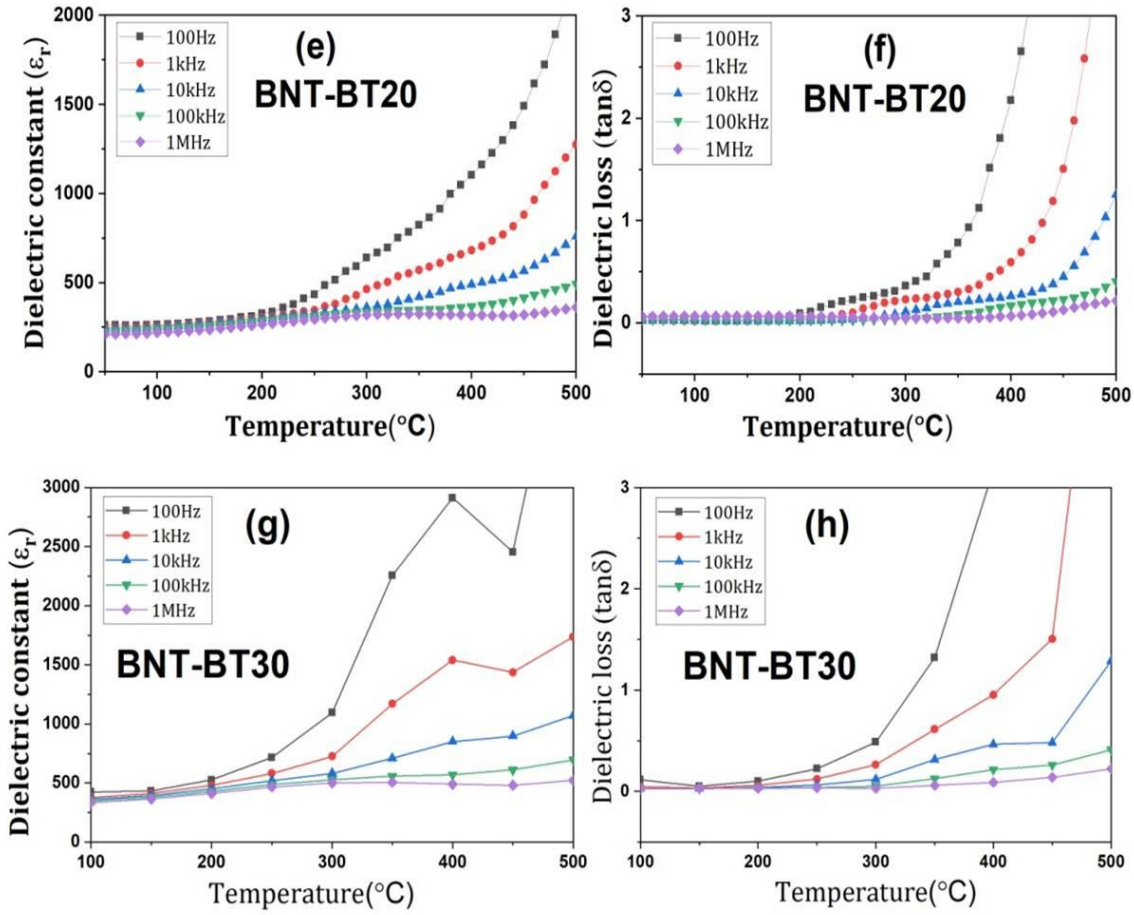

Figure 4.4: Plots of Dielectric constant and Dielectric loss with different temperature for BNT-BT0 , BNT-BT10 , BNT-20BT, and BNT-30BT ceramics

Variation of dielectric constant (ε_r) and tangent loss (tanδ) with frequency at different temperatures (200 ℃ - 450 ℃) have been shown in Figure 4.5(a-h) and the inset of Figure 4.5 shows the dielectric constant and tangent loss at low temperatures. It was found that dielectric constant and dielectric loss decreases with the rise in frequency and reaches a constant limit. The high dielectric constant in the low-frequency range than the high-frequency region is due to the space charge polarization. The tangent loss is relatively larger in low-frequency range than high-frequency zone. At higher temperature, the tangent loss is increased due to the existence of some impurity phases in the sample [48].

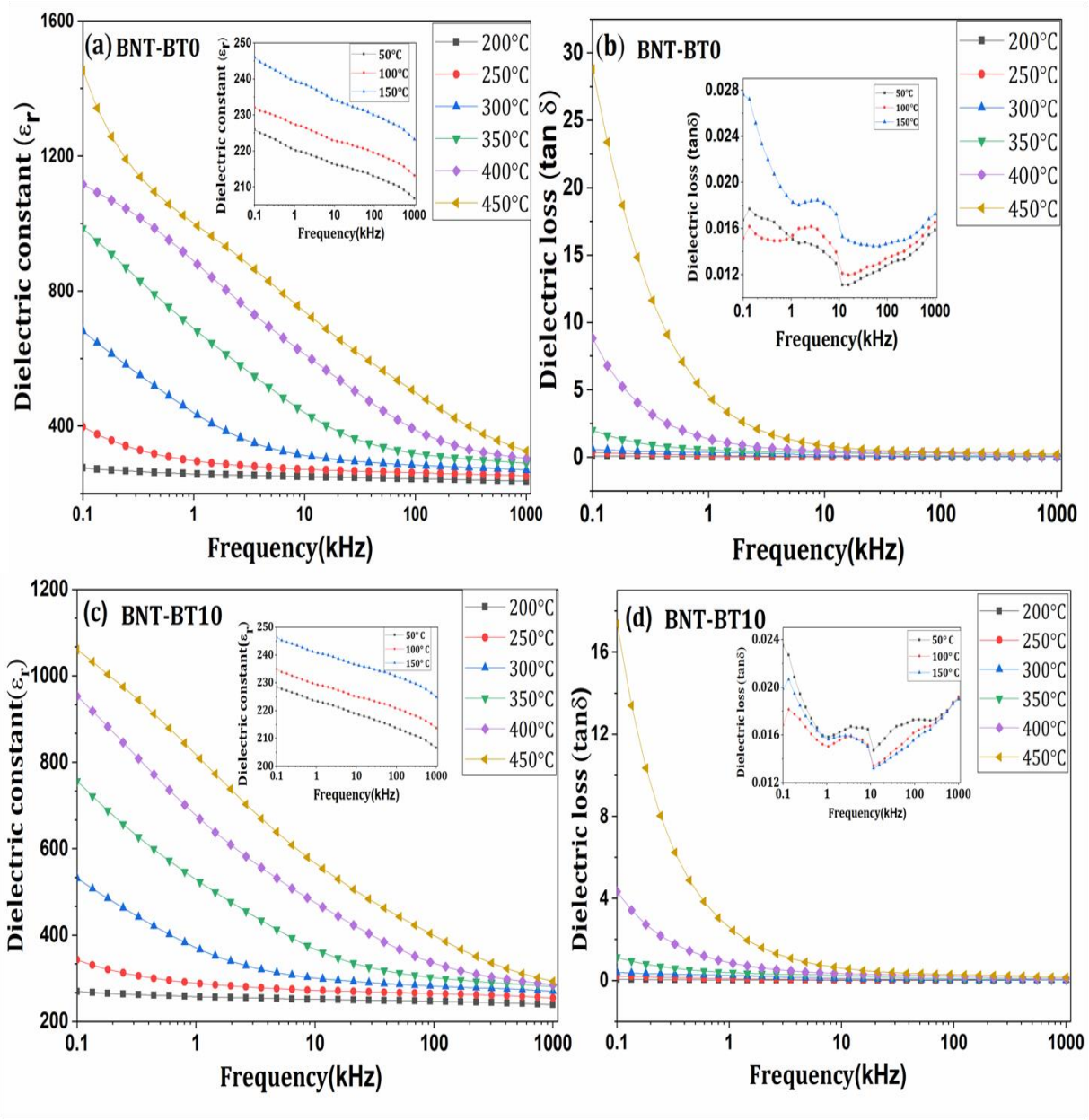
(a) BNT-BT0
Dielectric constant (ε_r)
Frequency(kHz)
200°C
250°C
300°C
350°C
400°C
450°C
50°C
100°C
150°C
(b) BNT-BT0
Dielectric loss (tan δ)
Dielectric loss (tanδ)
(c) BNT-BT10
Dielectric constant(ε_r)
(d) BNT-BT10

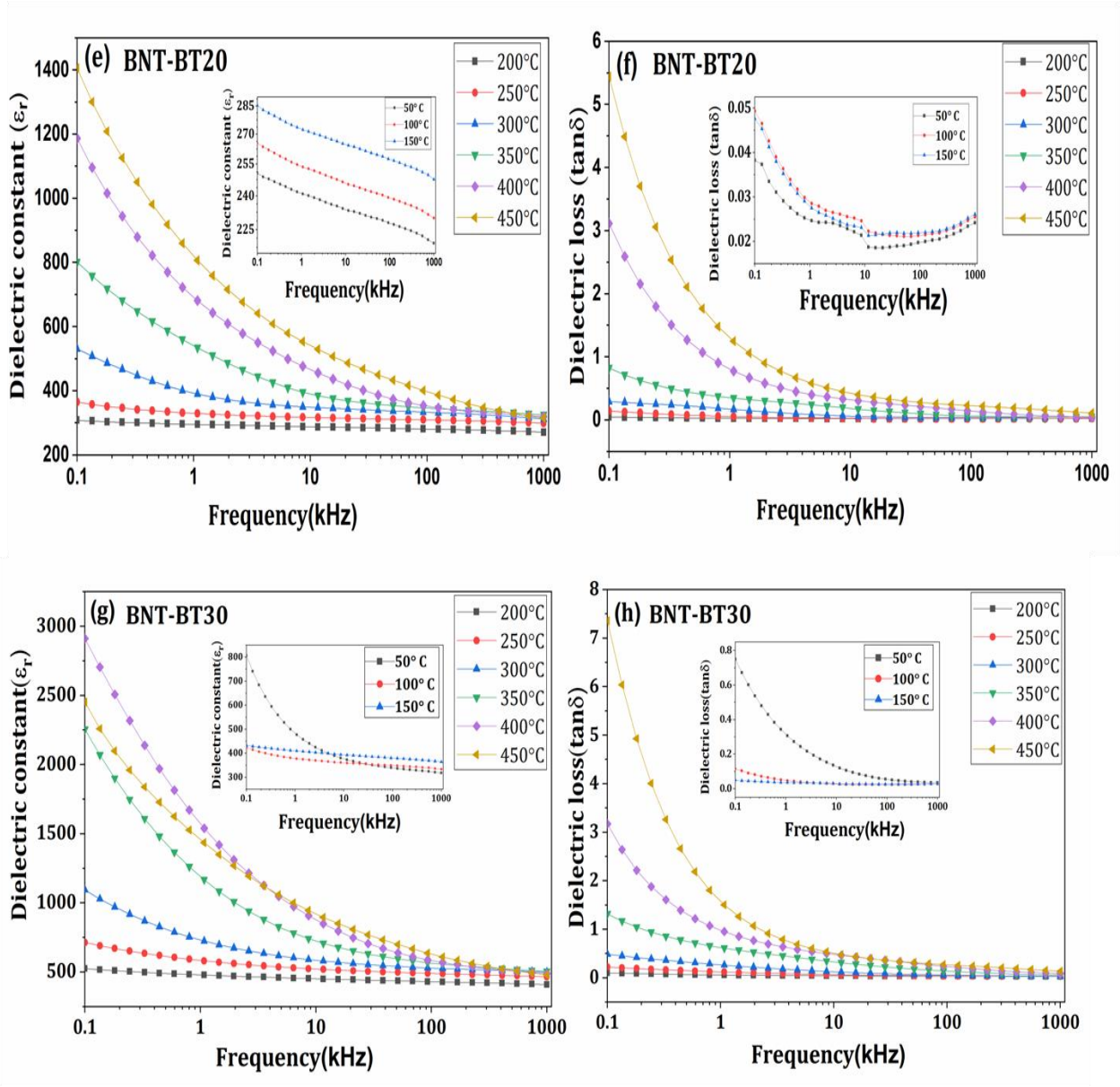

Figure 4.5: Plots of Dielectric constant and Dielectric loss with frequency dependence for BNT-BT0, BNT-BT10, BNT-BT20, and BNT-BT30 ceramics

4.4. Impendence analysis

Figure 4.6 (a-d) represents the frequency dependence of real component of impedance (Z') at various temperatures varying from 250 ºC to 500 ºC for BNT-BT0, BNT-BT10, BNT-BT20, and BNT-BT30. It is seen that real (Z') impedance decreases monotonically with increasing frequency upto 10 kHz, after that it becomes frequency-independent for all the samples.

Z'vs frequency plots show broadened peaks at lower frequency at higher temperature ranging from 400 ºC to 500 ºC (as shown in inset of Figure 4.6). At lower frequency, higher value of Z' indicate that polarization is larger in the compound and the value of Z' slightly decreases with increasing both frequency and temperature owing to space charge polarization. With increase the doping of $BaTiO_3$, the real part of impedance decreases slightly due to space charge polarization [48].

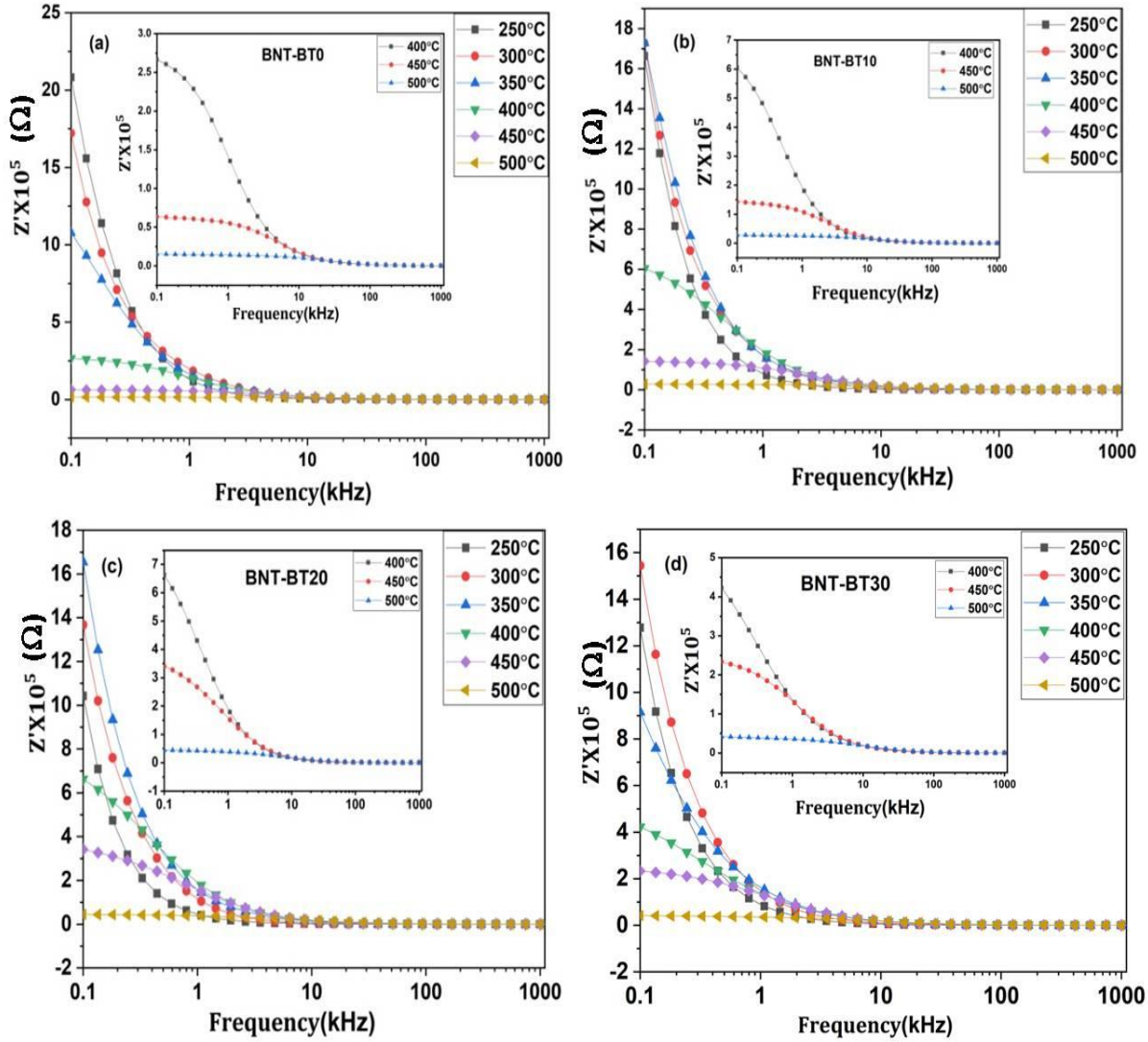

Figure 4.6: Z' vs. frequency of BNT-BT0, BNT-BT10, BNT-BT20, and BNT-BT30 ceramics

Figure 4.7 represents the frequency dependent imaginary component of impedance (Z") at several temperatures. The value of Z" is higher at lower frequencies, which shows the relaxation

process.The reason of the electrical relaxation process occurs due to defects or oxygen vacanices in the material. Similar behaviour is observed for all the compositions.The inset of the Figure 4.7 shows asymmetric broadening of peaks which shift towards the high-frequency region with increase in temperature.With increasing the Ba^{2+} amount, Z"increase except for 0.3 composition due to space charge polarization. **[48] [50]**

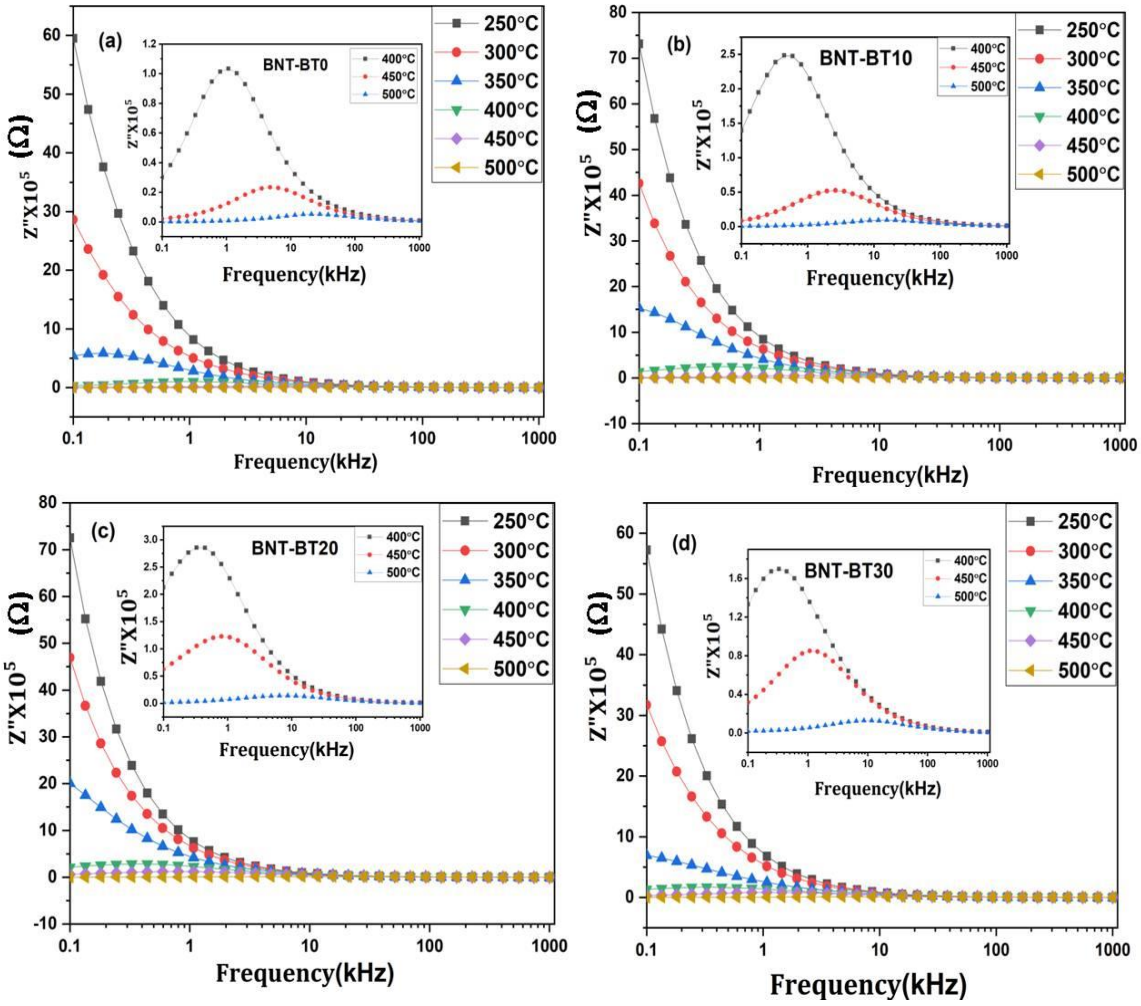

Figure 4.7: Z" vs. frequency of BNT-BT0, BNT-BT10, BNT-BT20, and BNT-BT30 ceramics

The Cole-Cole plot (Z" vs. Z') are taken at various temperature ranges from 250 ºC to 500 ºC(as shown in Figure 4.8). Semicircular arcs are observed in this spectrum. The radius of semicircle gradually decreases with the increase in temperature. It indicates that the bulk resistance of the material decreases and conductivity increases with increase in temperature. This signifies the

non-ideal Debye type behaviour and negative temperature coefficient of resistivity (NTCR) that may be due to the orientation of the grains boundary and defects [50-51]

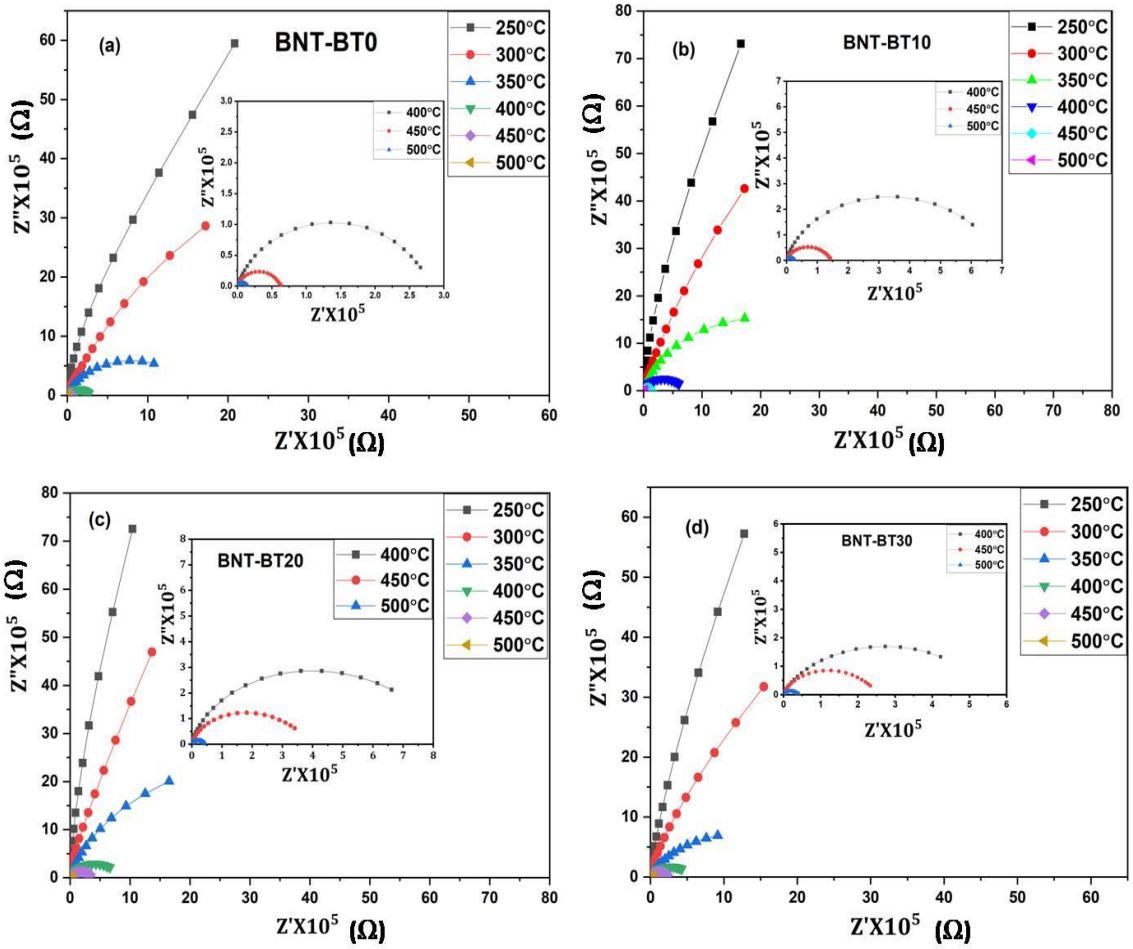

Figure 4.8: Z'' vs. Z' (Cole-Cole plot) of BNT-BT0, BNT-BT10, BNT-BT20, and BNT-BT30 ceramics

4.5. P-E loop Measurements

The room temperature P-E hysteresis loops of BNT and BNT-BT samples at maximum applied electric field are shown in Figure 4.9. The typical hysteresis loop were not observed because of the increase in concentration of Ba^{2+} resistivity of material decreases and conductivity increases, sample becomes overloaded due to coexistence of two phases and impurity in the sample. Therefore, the electric field cannot be applied. It is observed from figures that the values of remanent polarization (P_r) increase with the concentration of BT content. The maximum

polarization, remnant polarization, and coercive field value are shown in the following Table 4.10

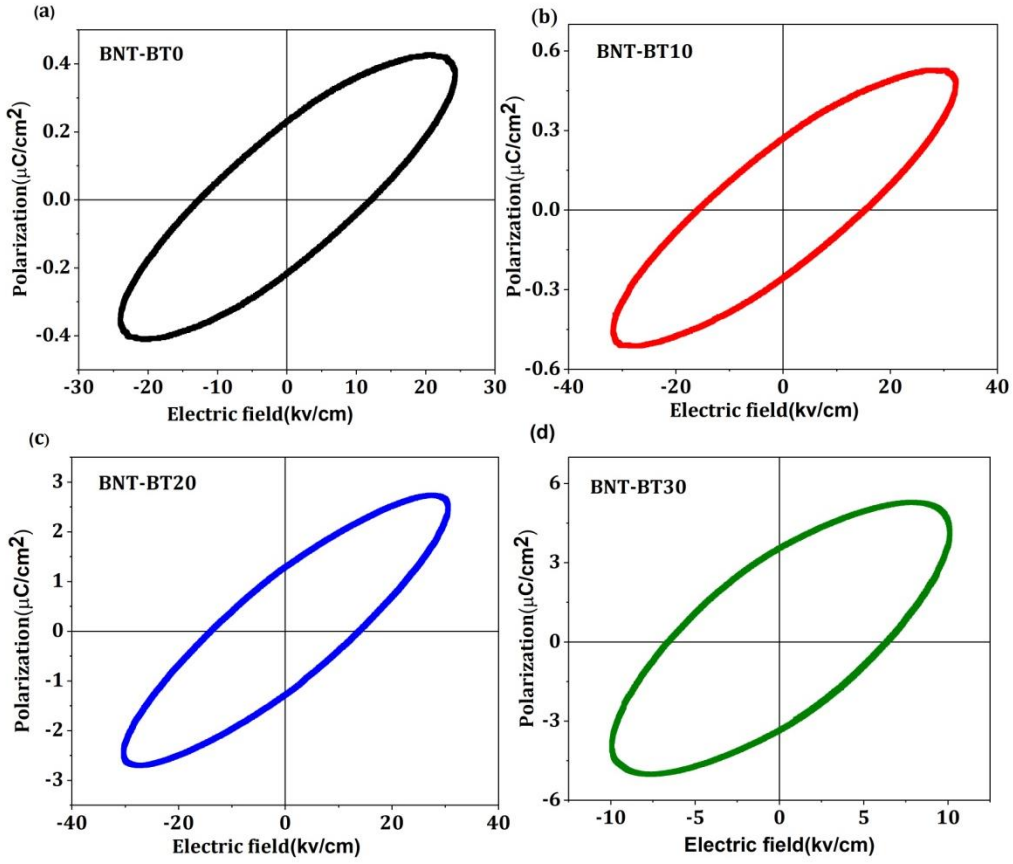

Figure 4.9: Room temperature P-E loop of BNT-BT0, BNT-BT10, BNT-BT20, and BNT-BT30 ceramics

Table 4.10 Ferroelectric properties of BNT-BT0, BNT-BT10, BNT-BT20, and BNT-BT30 ceramics

Sample name	Maximum polarization (in μC/cm^2)	Remnant polarization(P_r) (in μC/cm^2)	Coercive field (E_c) (in kV/ cm)
BNT- BT0	0.419	0.222	12.36
BNT- BT10	0.443	0.263	15.62
BNT- BT20	2.718	1.285	13.88
BNT- BT30	5.153	3.457	6.47

CHAPTER 5

CONCLUSION

5.1 Conclusion

A systematic study of structural, micro-structural, dielectric and ferroelectric properties of (1-x)BNT-xBT(x=0, 0.1, 0.2, and 0.3) ceramics have been reported. BNT-BTx ceramics were synthesized via conventionally solid-state method.

1. X-ray diffraction pattern showed the BNT-BTx series show coexistence of perovskite and aurivillus phase. This aurivillius phase is found to increase in $BaTiO_3$ content.The lattice parameters are found to increase with increase in $BaTiO_3$ concentration.
2. The SEM micrographs of the samples depict the non-uniform distribution of grains with unequal size.
3. The temperature dependent Dielectric constant and dielectric loss shows relaxor behaviour of all the samples.
4. Impedance studies should a decrease in the real impedance and increase in the imaginary value of impedance due to release of space charge polarization. From Cole-Cole plots studied that the bulk resistivity decrease with increase in the conductivity, it shows negative temperature coefficient nature of the ceramic.
5. The P-E Hysteresis loop shows that the remanent polarization is found to increase with increase in $BaTiO_3$ concentration and maximum polarization obtained is P_{max}= 5.153 $\mu C/cm^2$ for BNT-BT-30.

5.2 Suggestions for future work

The work done in the present dissertation is related to the study of ferroelectrics and dielectric properties of BNT. Following are the suggestions which can be opted for future research work:

1. The variation in dielectric and ferroelectric properties at different sintering temperatures can be done
2. Piezoelectric properties could be studied.
3. Studiesfor the higher concentration of $BaTiO_3$ could be done.

REFERENCES

1. Saito, Y., Takao, H., Tani, T., Nonoyama, T., Takatori, K., Homma, T., & Nakamura, M. (2004). Lead-free piezoceramics. *Nature*, *432*(7013), 84.
2. Gordon, J. N., Taylor, A., & Bennett, P. N. (2002). Lead poisoning: case studies. *British journal of clinical pharmacology*, *53*(5), 451-458.
3. Panda, P. K. (2009). Environmental friendly lead-free piezoelectric materials. *Journal of materials science*, *44*(19), 5049-5062.
4. Newnham, R. E. (1989). Electroceramics. *Reports on Progress in Physics*, *52*(2), 123.
5. Badr, A. M., Elshaikh, H. A., & Ashraf, I. M. (2011). Impacts of temperature and frequency on the dielectric properties for insight into the nature of the charge transports in the Tl2S layered single crystals. *Journal of Modern Physics*, *2*(01), 12.
6. FernandezBenavides, D., GutierrezPerez, A., BenitezCastro, A., AyalaAyala, M., Moreno Murguia, B., & MunozSaldana, J. (2018). Comparative study of ferroelectric and piezoelectric properties of BNT-BKT-BT ceramics near the phase transition zone. *Materials*, *11*(3), 361.
7. Subbarao, E. C. (1962). A family of ferroelectric bismuth compounds. *Journal of Physics and Chemistry of Solids*, *23*(6), 665-676.
8. Bhalla, A. S., Guo, R., & Roy, R. (2000). The perovskite structure- a review of its role in ceramic science and technology. *Materials research innovations*, *4*(1), 3-26.
9. Becker, M., Kluner, T., & Wark, M. (2017). Formation of hybrid ABX 3 perovskite compounds for solar cell application: first-principles calculations of effective ionic radii and determination of tolerance factors. *Dalton Transactions*, *46*(11), 3500-3509.
10. Niu, G., Guo, X., & Wang, L. (2015). Review of recent progress in chemical stability of perovskite solar cells. *Journal of Materials Chemistry A*, *3*(17), 8970-8980.
11. Vijatovic, M. M., Bobic, J. D., & Stojanovic, B. D. (2008). History and Challenges of Barium Titanate: Part I. *Science of Sintering*, *40*(2).
12. Vijatovic, M. M., Bobic, J. D., &Stojanovic, B. D. (2008). History and Challenges of Barium Titanate: Part II. *Science of Sintering*, *40*(3).
13. Jardiel, T., Caballero, A. C., & Villegas, M. (2008). Aurivillius ceramics: $Bi_4Ti_3O_{12}$-based piezoelectrics. *Journal of the Ceramic Society of Japan*, *116*(1352), 511-518.

14. Safari, A., Panda, R. K., & Janas, V. F. (1996). Ferroelectricity: Materials, characteristics & applications. *Key Engineering Materials 122*, 35-70.
15. Rotaru, A., & Morrison, F. D. (2015). Vogel–Fulcher analysis of relaxor dielectrics with the tetragonal tungsten bronze structure: $Ba_6MNb_9O_{30}$(M= Ga, Sc, In). *Journal of Thermal Analysis and Calorimetry*, *120*(2), 1249-1259.
16. Mandal, B. P., & Tyagi, A. K. (2010). Pyrochlores: Potential multifunctional materials. *Barc Newslett*, *313*, 6-13.
17. Sanson, A., & Whatmore, R. W. (2005). Phase Diagram of the $Bi_4Ti_3O_{12}$–$BaTiO_3$–($Na_{1/2}Bi_{1/2}$) TiO_3 System. *Journal of the American Ceramic Society*, *88*(11), 3147-3153.
18. Smolensky, G. A. (1961). New ferroelectrics of complex composition. IV. *Soviet Physics, Solid State*, *2*, 2651-2654.
19. Takenaka, T., Maruyama, K. I., & Sakata, K. (1991). ($Bi_{1/2}Na_{1/2}$) TiO_3-$BaTiO_3$ system for lead-free piezoelectric ceramics. *Japanese journal of applied physics*, *30*(9S), 2236.
20. Walsh, C. J., & Schulze, W. A. (2004, August). Bond valence structure analysis of doped bismuth sodium titanate. *International Symposium on Applications of Ferroelectrics, 2004. ISAF-04. 2004*, 328-331.
21. Sittiketkorn, P., & Bongkarn, T. (2013). Effects of sintering temperature on phase formation, microstructure and dielectric properties of BNT–BT ceramics prepared by combustion technique. *Ferroelectrics Letters Section*, *40*(4-6), 77-84.
22. Yang, Z., Hou, Y., Liu, B., & Wei, L. (2009). Structure and electrical properties of Nd_2O_3-doped0.82$Bi_{0.5}Na_{0.5}TiO_3$–0.18$Bi_{0.5}K_{0.5}TiO_3$ceramics. *Ceramics International*, *35*(4), 1423-1427.
23. Chu, B. J., Chen, D. R., Li, G. R., & Yin, Q. R. (2002). Electrical properties of $Na_{1/2}Bi_{1/2}TiO_3$–$BaTiO_3$ ceramics. *Journal of the European Ceramic Society*, *22*(13), 2115-2121.
24. Li, H. D., & Yao, W. L. (2004). Some effects of different additives on dielectric and piezoelectric properties of ($Bi_{1/2}Na_{1/2}$)TiO_3–$BaTiO_3$ morphotropic-phase-boundary composition. *Materials Letters*, *58*(7-8), 1194-1198.
25. Guo, Y., Kakimoto, K. I., & Ohsato, H. (2004). Structure and electrical properties of lead-free($Na_{0.5}K_{0.5}$) NbO_3-$BaTiO_3$ ceramics. *Japanese journal of applied physics*, *43*(9S), 6662.

26. Wang, C. M., Zhao, L., Wang, J. F., Zhang, S., & Shrout, T. R. (2009). Enhanced piezoelectric properties of sodium bismuth titanate ($Na_{0.5}Bi_{4.5}Ti_4O_{15}$) ceramics with B- site cobalt modification. *Physica status solidi (RRL)–Rapid Research Letters*, *3*(1), 7-9.
27. Zhao, M. L., Wu, Q. Z., Wang, C. L., Zhang, J. L., Gai, Z. G., & Wang, C. M. (2009). Dielectric and piezoelectric properties of $Na_{0.5}Bi_{4.5}Ti_4O_{15}$–$(x- 1)Na_{0.5}Bi_{0.5}TiO_3$ composite ceramics. *Journal of Alloys and Compounds*, *476*(1-2), 393-396.
28. Wang, C. M., Wang, J. F., Zhang, S., & Shrout, T. R. (2009). Electromechanical properties of A-site (LiCe)-modified sodium bismuth titanate ($Na_{0.5}Bi_{4.5}Ti_4O_{15}$) piezoelectric ceramics at elevated temperature. *Journal of Applied Physics*, *105*(9), 094110.
29. Rout, D., Moon, K. S., Rao, V. S., & Kang, S. J. L. (2009). Study of the morphotropic phase boundary in the lead-free $Na_{1/2}Bi_{1/2}TiO_3$-$BaTiO_3$ system by Raman spectroscopy. *Journal of the Ceramic Society of Japan*, *117*(1367), 797-800.
30. Cernea, M., Andronescu, E., Radu, R., Fochi, F., & Galassi, C. (2010). Sol–gel synthesis and characterization of $BaTiO_3$-doped $(Bi_{0.5}Na_{0.5})TiO_3$ piezoelectric ceramics. *Journal of Alloys and Compounds*, *490*(1-2), 690-694.
31. Ahn, C. W., Kim, I. W., Ha, M. S., Seo, W. K., Lee, J. S., & Yi, S. S. (2002). Dielectric and Piezoelectric Properties of Lead-Free $Na_{0.5}Bi_{4.5}$- $xLaxTi_4O_{15}$ and $Na_{0.5}Bi_{4.5}$-$xNdx$ Ti_4O_{15} Ceramics. *Ferroelectrics*, *273*(1), 261-266.
32. Gao, D., Kwok, K. W., & Lin, D. (2011). Microstructure, piezoelectric and ferroelectric properties of Mn-added $Na_{0.5}Bi_{4.5}Ti_4O_{15}$ ceramics. *Current Applied Physics*, *11*(3), S124-S127.
33. Sun, Y., Liu, H., Hao, H., Zhang, S., Guo, L., & Yu, Z. (2012). Effect of $Na_{0.5}Bi_{0.5}TiO_3$ on dielectric properties of $BaTiO_3$ based ceramics. *Ceramics International*, *38*, S41-S44.
34. Parija, B., Badapanda, T., Panigrahi, S., & Sinha, T. P. (2013). Ferroelectric and piezoelectric properties of (1-x)$(Bi_{0.5}Na_{0.5})TiO_3$-$xBaTiO_3$ ceramics. *Journal of Materials Science: Materials in Electronics*, *24*(1), 402-410.
35. Jiang, X. P., Fu, X. L., Chen, C., Tu, N., Xu, M. Z., Li, X. H., & Chen, Y. J. (2015). High performance Aurivillius type $Na_{0.5}Bi_{4.5}Ti_4O_{15}$ piezoelectric ceramics with neodymium and cerium modification. *Journal of Advanced Ceramics*, *4*(1), 54-60.

36. Hussin, A., Maqbool, A., Malik, R. A., Kim, M. S., Song, T. K., Kim, M. H., ... & Kim, W. J. (2015). Structural and Electrical Properties of $Bi_{0.5}Na_{0.5}TiO_3$ Templates Produced by Topochemical Microcrystal Conversion Method. *New Physics*, *65*(8), 715-720.
37. Jiang, X. P., Jiang, X. A., Chen, C., Tu, N., Chen, Y. J., & Zhang, B. C. (2016). Effect of potassium sodium niobate (KNN) substitution on the structural and electrical properties of $Na_{0.5}Bi_{0.5}Ti_4O_{15}$ ceramics. *Journal of Physics D: Applied Physics*, *49*(12), 125101.
38. Shamim, M. K., Sharma, S., Sinha, S., & Nasreen, E. (2017). Dielectric relaxation and modulus spectroscopy analysis of ($Na_{0.47}K_{0.47}Li_{0.0\ 6}$) NbO_3 ceramics. *Journal of Advanced Dielectrics*, *7*(03), 1750020.
39. Zhang, C. C., Zou, J. X., Li, L. H., Luo, Q., Ma, C., Gui, L.,& Ding, Y. M. (2017). Dielectric and ferroelectric properties of bismuth-layer high Curie point $Na_{0.5}Bi_{4.5}Ti_4O_{15}$ ceramics with Mg-doping. *Ceramics International*, *43*(16), 13963-13969.
40. Sahoo, S., Hajra, S., De, M., & Choudhary, R. N. P. (2018). Resistive, capacitive and conducting properties of $Bi_{0.5}Na_{0.5}TiO_3$-$BaTiO_3$ solid solution. *Ceramics International*, *44*(5), 4719-4726.
41. Liu, G., Wang, Z., Zhang, L., Shi, W., Jing, J., Chen, Y., & Yan, Y. (2018). Phase segregation and dielectric, ferroelectric, and piezoelectric properties of MgO-doped NBT-BT lead-free ferroelecric ceramics. *Materials Research Express*, *5*(3), 036305.
42. Hajra, S., Sahoo, S., Das, R., & Choudhary, R. N. P. (2018). Structural, dielectric and impedance characteristics of $(Bi_{0.5}Na_{0.5})TiO_3$-$BaTiO_3$ electronic system. *Journal of Alloys and Compounds*, *750*, 507-514.
43. Munir, M., Habib, M., Khan, S. A., Hussain, A., Qazi, I., Choi, Y. B.,& Bae, D. S. (2019). Effect of the processing temperature on the electrical properties of lead-free 0.965 $Bi_{0.5}Na_{0.5}TiO_3$-0.035$BaTiO_3$ piezoelectric ceramics synthesized by sol–gel method. *Journal of Sol-Gel Science and Technology*, *90*(3), 643-652.
44. Jiang, C., Ma, C., Luo, Q., Liu, K., Qin, L., Wu, Z., & Chen, Y. (2019). Piezoelectric and ferroelectric properties of $Na_{0.5}Bi_{4.5}Ti_4O_{15}$-$BaTiO_3$ composite ceramics with Mg doping. *Journal of Advanced Dielectrics*, *9*, 1-6.
45. Munir, M., Hussain, A., Ock, J. Y., Son, J. H., Khan, S. A., & Bae, D. S. (2019). Structure Analysis and Ferroelectric Response of $Bi_{0.5}Na_{0.5}TiO_3$ Nanopowder Synthesized by Sol–Gel Method. *Journal of nanoscience and nanotechnology*, *19*(3), 1323-1329.

46. Turki, O., Slimani, A., Seveyrat, L., Sassi, Z., Khemakhem, H., & Lebrun, L. (2019). Enhancement of dielectric, piezoelectric, ferroelectric, and electrocaloric properties in slightly doped $(Na_{0.5}Bi_{0.5})0.94Ba_{0.06}TiO_3$ ceramic by samarium. *Journal of Applied Physics*, *125*(17), 174103.
47. Zhao, M. L., Wu, Q. Z., Wang, C. L., Zhang, J. L., Gai, Z. G., & Wang, C. M. (2009). Dielectric and piezoelectric properties of $Na_{0.5}Bi_{4.5}Ti_4O_{15}$-(x-1) $Bi_{0.5}Na_{0.5}TiO_3$ composite ceramics. *Journal of Alloys and Compounds*, *476*(1-2), 393-396.
48. Kumari, K., Prasad, A., & Prasad, K. (2016). Dielectric, Impedance/modulus and conductivity studies on [Bi 0.5(Na 1-x K x) 0.5] 0.94 Ba 0.06 TiO 3, [0.16 x 0.20] leadfree ceramics. *American Journal of Materials Science 6*(1), 1-18.
49. Hajra, S., Sahoo, S., Das, R., & Choudhary, R. N. P. (2018). Structural, dielectric and impedance characteristics of $(Bi_{0.5}Na_{0.5})TiO_3$–$BaTiO_3$ electronic system. *Journal of Alloys and Compounds*, *750*, 507-514.
50. Acharya, T., & Choudhary, R. N. P. (2015). Dielectric behavior of manganese titanate in the paraelectric phase. *Applied Physics A*, *121*(2), 707-714.
51. Thakur, S., Rai, R., Bdikin, I., & Valente, M. A. (2016). Impedance and modulus spectroscopy characterization of Tb modified $Bi_{0.8}A_{0.1}Pb_{0.1}Fe_{0.9}Ti_{0.1}O_3$ ceramics. *Materials Research*, *19*(1), 1-8.

Turnitin Originality Report

Processed on: 15-Jul-2019 12:57 +0530
ID: 1152006563
Word Count: 6036
Submitted: 1

anjali mehta thesis v02 By Anjali Mehta`

Similarity Index	Similarity by Source	
13%	Internet Sources:	4%
	Publications:	6%
	Student Papers:	9%

1% match (student papers from 27-May-2019)
Submitted to Visvesvaraya National Institute of Technology on 2019-05-27

1% match (publications)
Sushrisangita Sahoo, Sugato Hajra, Manojit De, R.N.P. Choudhary. "Resistive, capacitive and conducting properties of Bi 0.5 Na 0.5 TiO 3 -BaTiO 3 solid solution", Ceramics International, 2018

1% match (publications)
Jiagang Wu, Dingquan Xiao, Jianguo Zhu. "Potassium–Sodium Niobate Lead-Free Piezoelectric Materials: Past, Present, and Future of Phase Boundaries", Chemical Reviews, 2015

1% match (student papers from 11-Apr-2017)
Submitted to University of Sheffield on 2017-04-11

1% match (student papers from 12-May-2014)
Submitted to National Institute of Technology, Rourkela on 2014-05-12

1% match (student papers from 02-Oct-2015)
Submitted to University of Ulsan on 2015-10-02

1% match (student papers from 12-May-2014)
Submitted to National Institute of Technology, Rourkela on 2014-05-12

< 1% match (student papers from 11-Feb-2014)
Submitted to Higher Education Commission Pakistan on 2014-02-11

< 1% match (Internet from 11-Jul-2019)
https://aip.scitation.org/doi/10.1063/1.2816118

< 1% match (Internet from 25-Sep-2015)
http://worldwidescience.org/topicpages/0-9/0-3+ferroelectric+composites.html

< 1% match (student papers from 23-Nov-2016)
Submitted to University of the Phillipines on 2016-11-23

< 1% match (student papers from 31-Oct-2016)
Submitted to National Institute of Technology, Rourkela on 2016-10-31

< 1% match (student papers from 23-Nov-2018)
Submitted to Universiti Teknologi MARA on 2018-11-23

< 1% match (student papers from 13-May-2016)
Submitted to University of Hull on 2016-05-13

< 1% match (publications)
Sharma, Dhananjay K., Nawnit Kumar, Seema Sharma, and Radheshyam Rai. "Effect of BaTiO3 additive on the electrical properties of Na0.50Bi0.50TiO3 lead free ceramics", Materials Chemistry and Physics, 2013.

< 1% match (student papers from 09-Jan-2013)
Submitted to Indian Institute of Technology Roorkee on 2013-01-09

< 1% match (student papers from 05-Jul-2019)
Submitted to Pandit Deendayal Petroleum University on 2019-07-05

< 1% match (Internet from 17-Apr-2019)
https://research-repository.st-andrews.ac.uk/bitstream/handle/10023/4184/AndreiRotaru_PhDThesis.PDF?isAllowed=y&sequence=6

< 1% match (Internet from 09-Mar-2016)
http://ethesis.nitrkl.ac.in/4659/1/Ph.D_Thesis-507PH005-_S_Naresh_Kumar.pdf

< 1% match (Internet from 04-May-2019)
https://link.springer.com/article/10.1007%2Fs10973-014-4355-5

< 1% match (Internet from 17-Apr-2019)
http://www.krishisanskriti.org/vol_image/21Jan201607012946%20%20%20%20%20%20%20%20Rajveer%20Singh%20%20%20%20%20%1940.pdf

< 1% match (student papers from 20-Jan-2011)
Submitted to University of Hong Kong on 2011-01-20

< 1% match (publications)
Zheng, X.H.. "Crystal structure and dielectric properties of ferroelectric ceramics in the BaO-Sm"2O"3-TiO"2-Nb"2O"5 system", Solid State Communications, 200302

< 1% match (publications)